CHALMERS

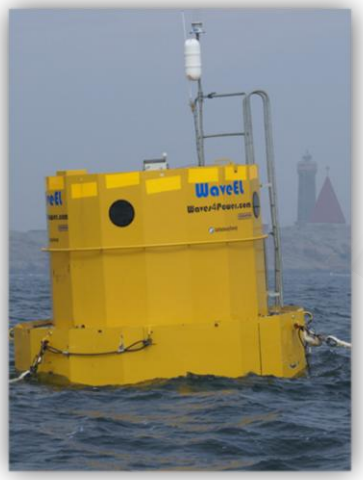

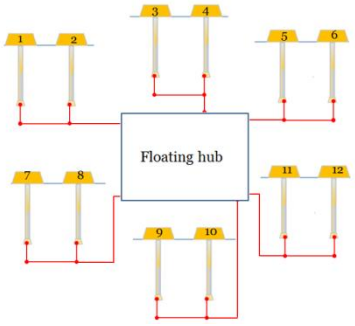

ELECTRICAL SYSTEM FOR WAVEFARM

Master of Science Thesis in Electric Power Engineering

MUHAMMAD ADNAN AZMAT

DIVISION OF ELECTRIC POWER ENGINEERING
DEPARTMENT OF ENERGY AND ENVIRONMENT
CHALMERS UNIVERSITY OF TECHNOLOGY
GÖTEBORG, SWEDEN

ELECTRICAL SYSTEM FOR WAVEFARM

Master of Science Thesis in Electric Power Engineering

MUHAMMAD ADNAN AZMAT

Department of Energy and Environment
Division of Electric Power Engineering
CHALMERS UNIVERSITY OF TECHNOLOGY
Göteborg, Sweden

Electrical System for Wavefarm

Master of Science Thesis in Electric Power Engineering
MUHAMMAD ADNAN AZMAT

Department of Energy and Environment
Division of Electric Power Engineering
Chalmers University of Technology
SE-412 96 Göteborg
Sweden
Telephone: + 46 (0)31-772 1000

Cover: Wave El Buoy [1], ABB´s SyncRM [2], ABB Frequency Converter [3] [4], 6-radial scheme

I DEDICATE THIS THESIS WORK TO MY BELOVED PARENTS

AKNOWLEDGEMENTS

I would like to express my heartiest appreciation to my supervisor ***Carl Ejnar Sölver*** from ***Waves4Power AB***, without whose assistance and support this thesis work would not have been successful. His kind guidance and active assistance enabled me to achieve the goal.

I would like to thank ***Per Halvarsson*** from ***ABB Corporate Research Västerås*** whose technical assistance helped me to grasp the practicality of the project. I also thank him for arranging the meetings and discussions during the course of the project.

I would like to thank my Examiner, ***Ola Carlson*** at ***Chalmers University of Technology*** for his support and help during the project.

I would like to say thanks to ***Henri Putto*** from ***ABB Mölndal*** and ***Hector Zelaya De La Parra*** from ***ABB, Corporate Research Västerås*** for their contribution and interest in the project.

I would like to express my gratitude to ***Göran Fredrikson*** from ***Waves4Power AB*** for providing me an opportunity to work for ***Waves4Power AB.*** I would like to thank ***Gunnar Fredrikson*** to attend the presentation seminar at ***Waves4power AB.***

I am grateful to the entire Faculty in ***Division of Electric Power Engineering*** for enhancing my knowledge and providing me a chance to enjoy studying in a multi-cultural and skill oriented environment at ***Chalmers University of Technology.***

Thanks to my colleagues ***Arslan Ashraf*** for his assistance and ***Gloria Puglia*** for opposing at the final thesis seminar. Many thanks to all other friends and colleagues for their support and encouragement throughout the project.

Last but not the least special thanks to my dear Father ***Azmat Ali***, my sweet mother ***Yasmin Azmat*** my brothers, ***Usman***, ***Salman*** and ***Azan*** for being supportive and encouraging me in every moment of my life.

Muhammad Adnan Azmat
GÖTEBORG, SWEDEN.
December, 2012

Electrical System for Wavefarm
Master of Science Thesis in Electric Power Engineering

MUHAMMAD ADNAN AZMAT
Department of Energy and Environment
Division of Electric Power Engineering
Chalmers University of Technology
Göteborg, Sweden

ABSTRACT

Electrical power production through renewable energy sources has gained importance over last few decades due to depleting natural resources and increasing concerns about green energy. Replacing the use of fossil fuels, coal, oil, and natural gas; renewable energy sources can deliver the growing demand of electricity. Wave energy is one of the emerging and promising renewable energy source that can potentially contribute in delivering electrical power.

In this project electrical design of a wavefarm comprising of various wave energy converters was proposed. In this regard the design of wave energy converter (Wave El Buoy) was studied. Economically and practically feasible design is selected for a single buoy unit. Performance of Wave El Buoy was evaluated by considering Synchronous reluctance generator and full power frequency converter. Standard components were employed to achieve cost effectiveness ensuring the system reliability. Additionally, the integration of this system into the floating transformer hub considering various radial schemes was investigated based on performance and economics. This included power loss evaluation of the transmission network and the voltage drop over each radial scheme. Optimal design with lowest power loss and voltage drop was selected and proposed. Lastly in this project, in order to understand the potential of wave energy, a comparison was made between a wavefarm and a windfarm in terms of power density.

Contents

List of Figures

List of Tables

1. Introduction

Wave power is the potential and kinetic energy associated with the ocean waves and transformation of this energy into useful form of work. Waves are caused by the wind as it blows across the sea bed. Gravitational force and the sea surface tension are also involved in the wave formation [5]. This can be visualized in the figure below

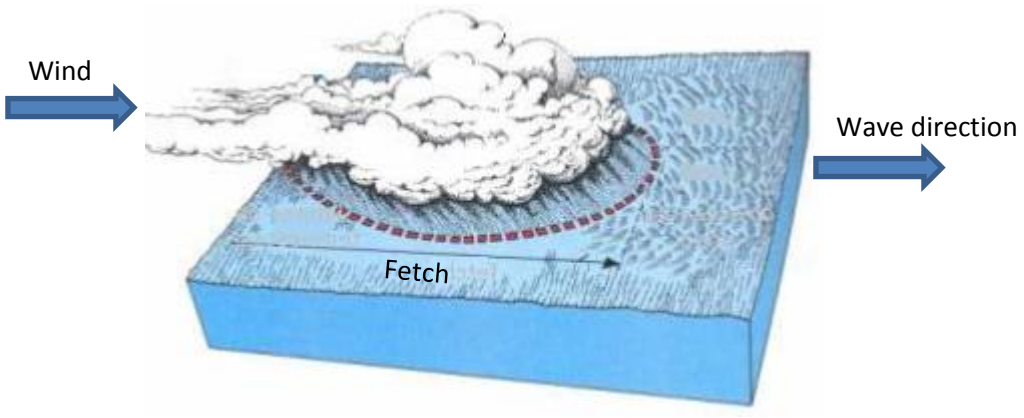

Figure 1: Wave formation in a Sea [5]

The mechanical power associated with wave of wavelength λ, height H, and wave front b is given by [5]

$$P = \frac{1}{2}\rho g H^2 \lambda b \; W \tag{1.1}$$

Where

ρ=specific weight of water
g=force of gravity

There are different methodologies to convert the energy contained in the waves into useful work. The kinetic and potential energy in the waves can be converted to electrical energy. This is conversion can be achieved with the wave energy converter discussed later.

1.1 Global wave power potential

Wave energy potential across the globe is very promising. This can be observed in the following figure

Figure 2: Global wave energy potential [6]

The wave energy potential is diverse as can be observed in the figure above. The energy density is related to location of the waves. Off shore location offers higher energy density as compared to near shore location. This shows that the energy extraction is dependent on the location. Moreover, the wave energy potential across the shores in Europe also inspires the research in wave energy extraction.

There is a limitation to harness this wave energy and convert it into electricity in large amounts. Hence there are certain drawbacks:

1. Electrical generation or the output is very variable.
2. Design of the device must be rigid enough to with stand the intense climate in the sea.
3. It requires a lot of feasibility study to select an appropriate location to install the device.
4. Selection of the suitable conversion scheme to extract maximum energy.

There is a challenge of efficiently capturing this irregular motion also has an impact on design of the device. To operate efficiently, the device and the corresponding systems have to most common wave power levels. Thus it is possible to gain maximum efficiency out of the system. Another challenge is the anchoring system for the device. It is essential to keep the device steady in place so that the device doesn't lose its position while it is in operation and the anchoring system needs to be tough enough to withstand the storm and intense climatic conditions in a sea or ocean. It is important here to mention that the anchoring system depends upon the wave energy conversion scheme. When a wave energy converter runs at wave conditions below what it is designed for, called part-load operation. Similarly when the wave condition

exceeds the design then it is called the over-load operation. The overload could lead to significant structural damage. Thus the load condition is unavoidable for a wave energy converter.

1.2 Wave Energy Converter

1.2.1 Operating principles

There are three main operating principles for a wave energy converter principle:

- **Oscillating water column (OWC)**

These devices use wave action to expand and compress air above a water column, to rotate and turbine or a generator.

- **Overtopping Devices (OTD)**

In this type of device the wave spills over into a reservoir, elevating the water above the sea level so that it can be used to run a low-head hydro turbine, i-e., Kaplan turbine

- **Wave Activated Bodies (WAB)**

This device oscillates due to a wave action relative to a fixed reference or to other parts of body.

1.2.2 Directional characteristics

There are three main directional characteristics for a wave energy converter

- **Point Absorbers**

These floating devices have dimensions that are relative to the incident wave length. They can capture wave energy from wave front that is larger than the dimensions of the absorber. These devices absorb energy from all directions.

- **Terminator**

The principle axis of this device is aligned perpendicular to the direction of wave propagation and in essence `terminates` the wave action. The waves are produced which are exactly in anti-phase with the incident waves.
Wave dragon is an example of the terminator.

- **Attenuator**

The principle axis of this device id aligned parallel or in the direction of wave propagation and in essence `attenuates` or reduces the amplitude of the wave.

1.3 WaveEL Buoy

The device used in the project is called WaveEL Buoy. The buoy can be observed in the figure below:

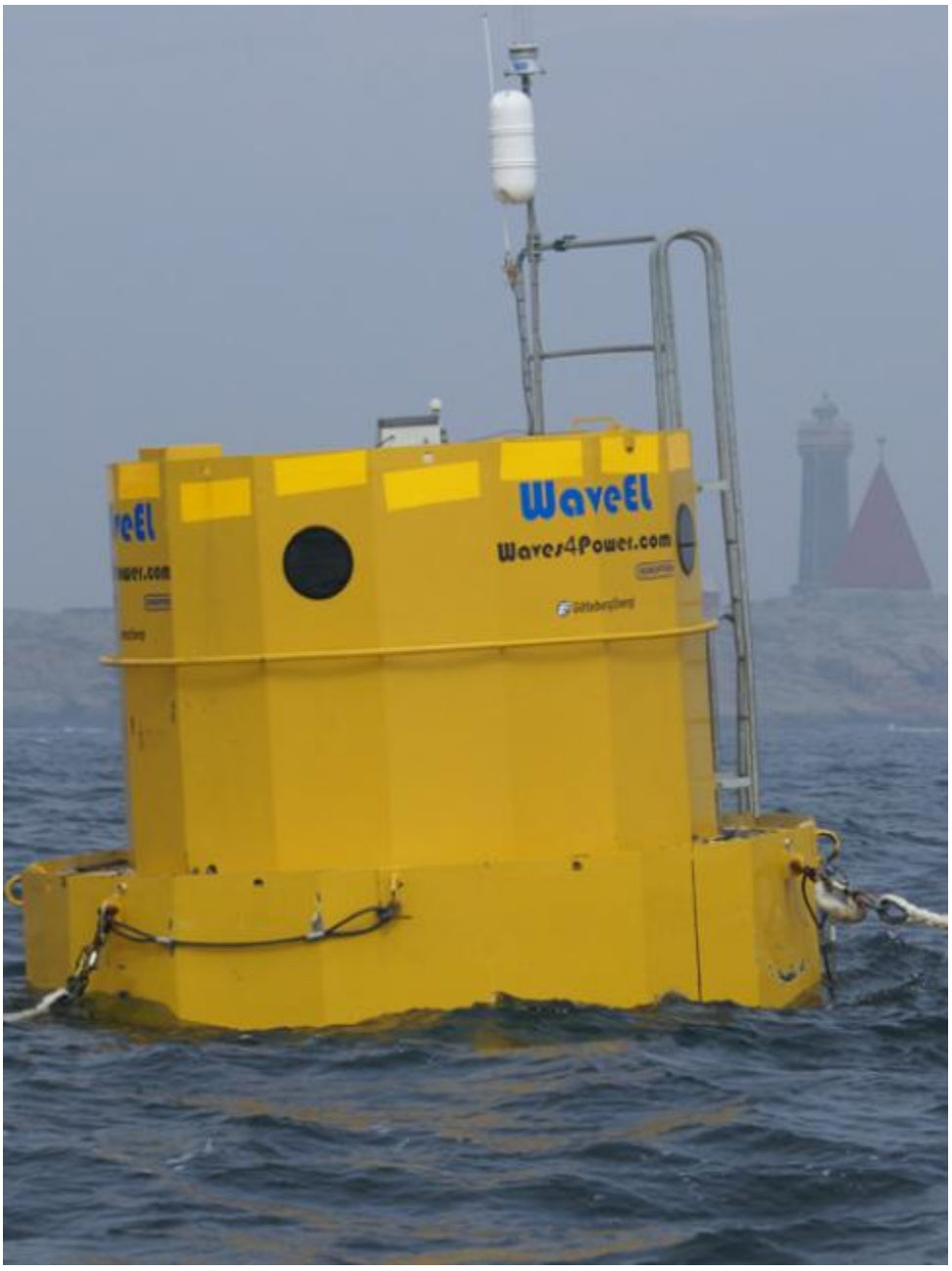

Figure 3: WaveEL Buoy [1]

The generator and the converter are placed inside the buoy and will be given in details further.

1.3.1 Working principle of WaveEL Buoy

The WaveEL Buoy consists of the following parts:

- Buoy body.
- Acceleration tube.
- Water piston.
- Concrete anchors.
- Hydraulic motor.
- Electrical generator.
- Polyester rope.

The construction of Wave El Buoy can be observed in the following figure

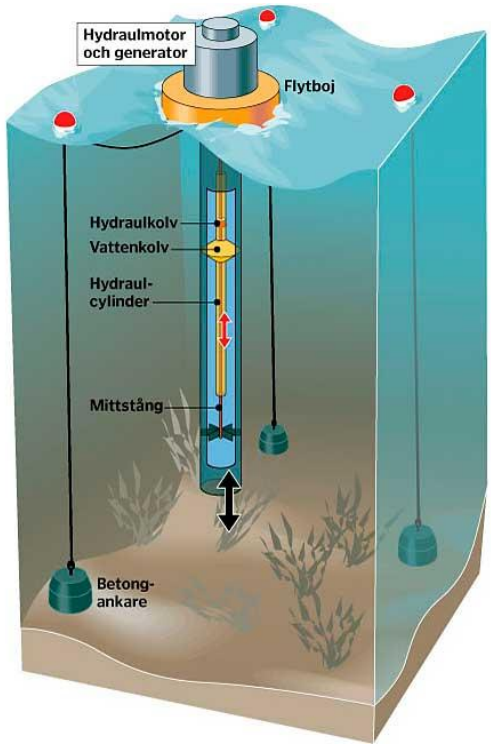

Figure 4 Parts of the buoy

- The acceleration tube passed through the buoy. Water piston inside the acceleration tube is connected to the hydraulic motor.
- Hydraulic motor is coupled with the electrical generator.
- The polyester ropes securing the buoy on station allowing free heaving motion.

The acceleration tube is suspended 25m deep in the water. The tube is open at both ends. When the tube is still, the water level inside the tube will be similar to the water level outside the buoy. There are two oscillating systems that can be visualized as follows

- The buoy and the acceleration tube
- The water mass present inside the acceleration tube

It is worthy to note that the motion of the buoy is opposite to that of the waves. This means that the buoy heaves down when the wave heaves up and vice versa. The water piston inside the acceleration tube is connected to the hydraulic piston. The energy is stored with the help of an accumulator and fed to the hydraulic motor which is coupled with the electrical generator. Figure 3 shows another view of the buoy and the mooring system which keeps the buoy in the position [1].

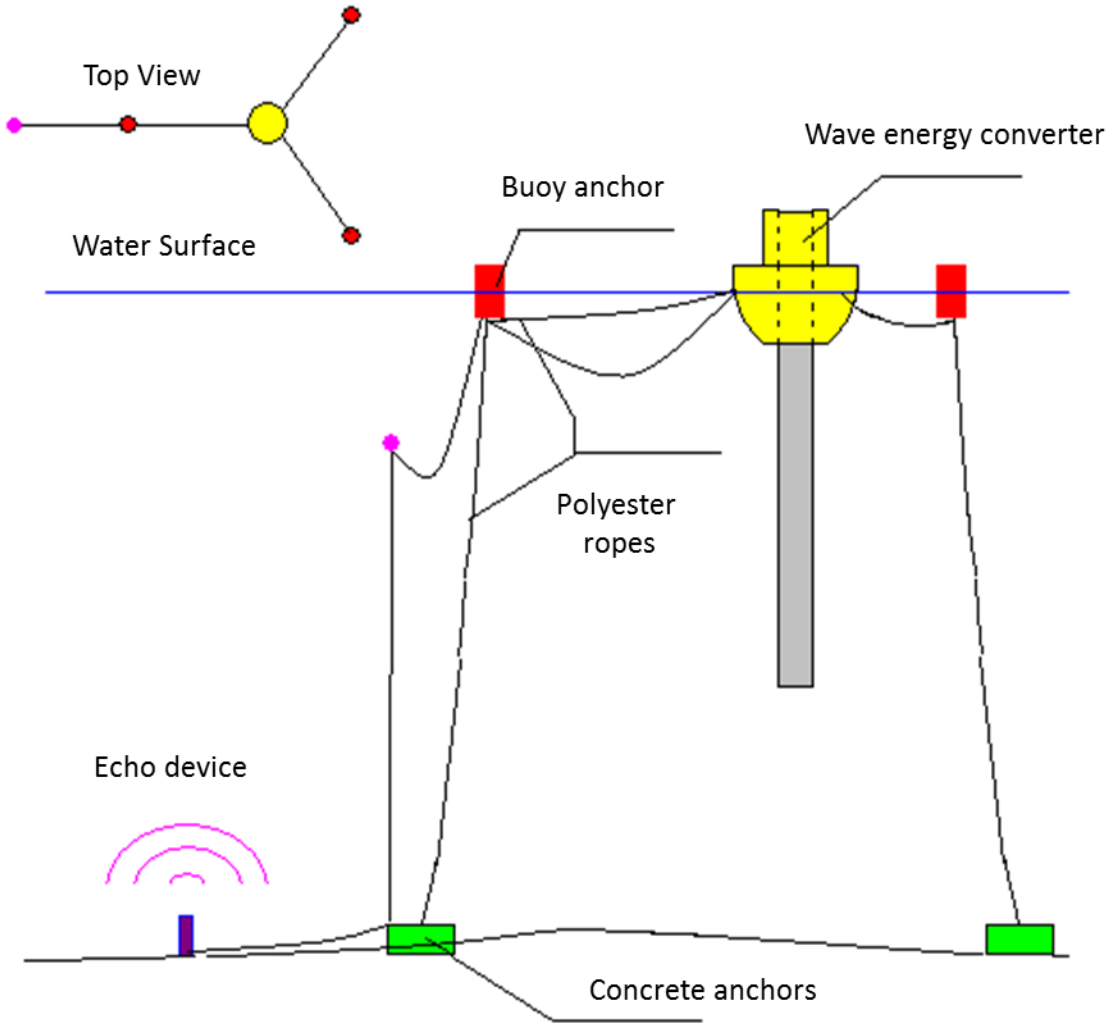

Figure 5: Mooring system of Wave El Buoy

2. Electrical energy from Wavefarm

In a wave energy converter and the buoy type discussed in the previous chapter, the hydraulic system is coupled with the electrical generator which produces the electrical energy. This energy is in a raw form and needs to be processed before transmission. The frequency of the generated power is variable, hence it is important to find a way to transform the energy into acceptable frequency level. For this purpose there are several topologies that can be taken into account for the conversion of the energy for the effective transportation.

2.1 Generic electrical system from buoys to the hub

In a wavefarm there are several buoys connected together and transmit the electrical energy to the transformer where it is stepped up and then transmitted further to the grid. The figure below shows the generic setup of the system.

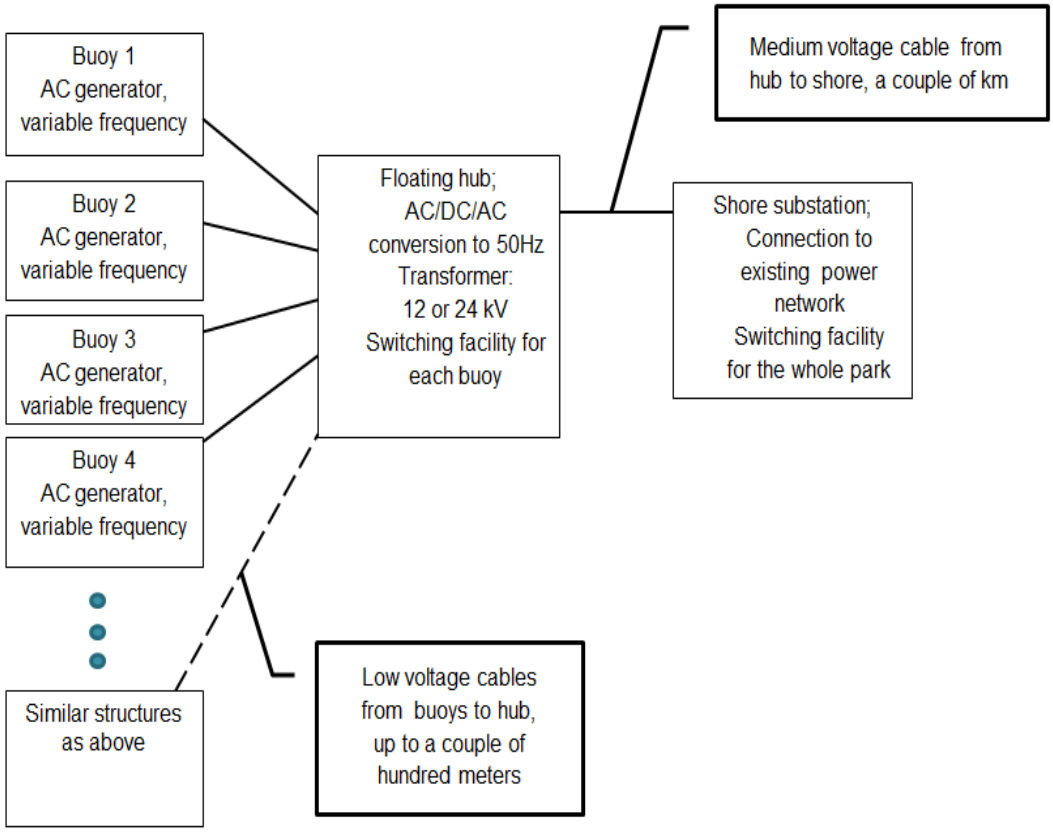

Figure 6: Generic electrical system

Figure 4 shows various buoys connected together and with the variable frequency link. The low voltage cables takes this produced electrical power to the floating hub where the transformer is installed. There could also be a conversion from AC- DC-AC depending upon the best available solution. The frequency is converted to 50 Hz. The transformer then steps up the voltage level to 12 kV or 24 kV. The medium voltage cables then take this stepped up power to the shore substation where it is connected the existing power network. Here it is important to note that the low voltage link between the different buoys and the floating substation consist of couple of hundred meters of cable. The medium voltage link between the floating hub and the shore sub-station consist of cables which could be some couple of kilometers in length.

2.2 Connection topologies

There are several connection topologies that can be taken into the account for the connection of the buoy with the floating transformer.

2.2.1 Power conversion both at the buoy and the floating transformer hub

In this type of topology the generated energy from the buoy is first rectified from AC to DC. The DC is then transmitted to the floating transformer hub where it is first inverted from DC to AC then fed into the transformer. It can be seen in the figure below

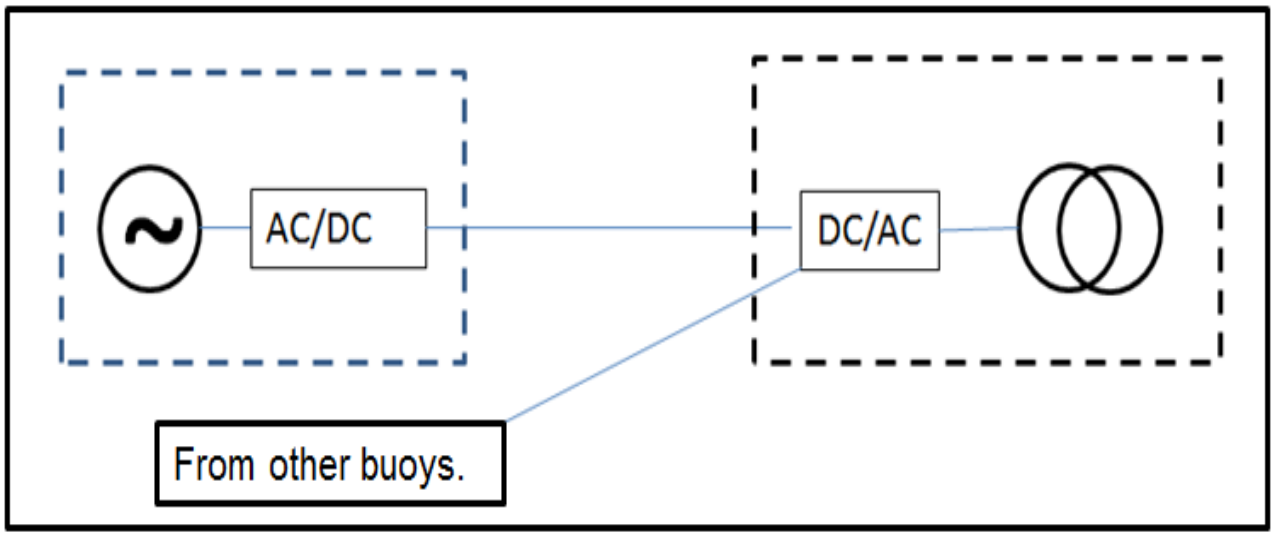

Figure 7: Two conversion stages of power

It can be observed that the other links would be similar to the first one and transmit the power to the transformer where it is first inverted.

2.2.2 Variable frequency link to the floating transformer hub

In this type of topology the power is not converted on the buoy. The variable frequency links are transmitted to the floating transformer hub where they are first rectified to DC and then inverted back to AC to obtain 50 Hz. This can be observed in the figure below

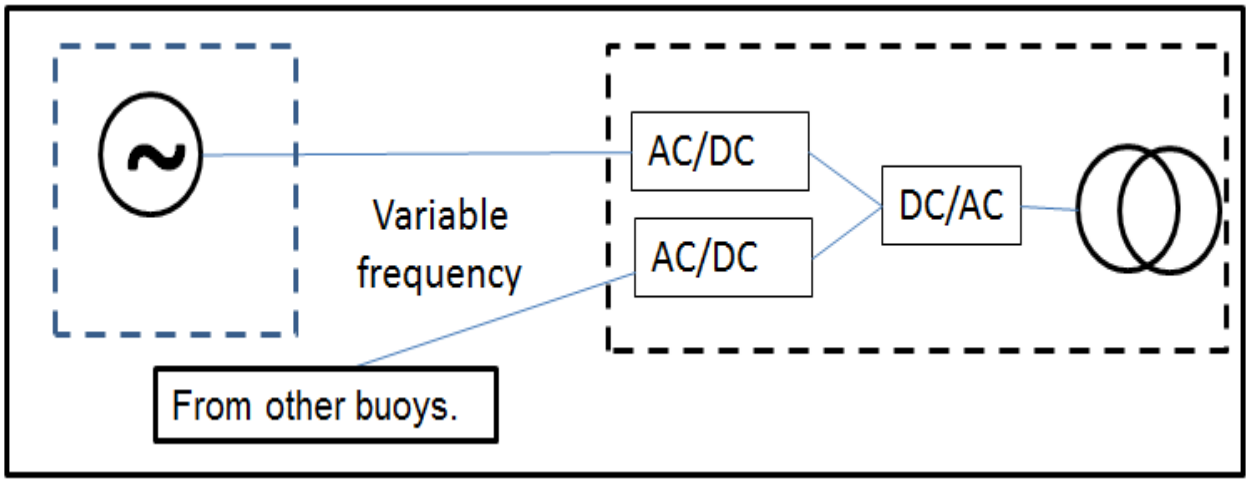

Figure 8: Variable frequency link

It can be observed in the above figure that the frequency from the various buoys is variable and not converted to 50 Hz. It is transmitted to the floating transformer hub where it is converted to 50 Hz AC using AC-DC-AC converter on the floating transformer hub.

2.2.3 50 Hz frequency link to the floating transformer hub

This topology is similar to that of the previous topology discussed above. Only the difference is that the AC-DC-AC conversion is done on each buoy before transmitting it to the floating transformer hub. This can be observed in the figure below

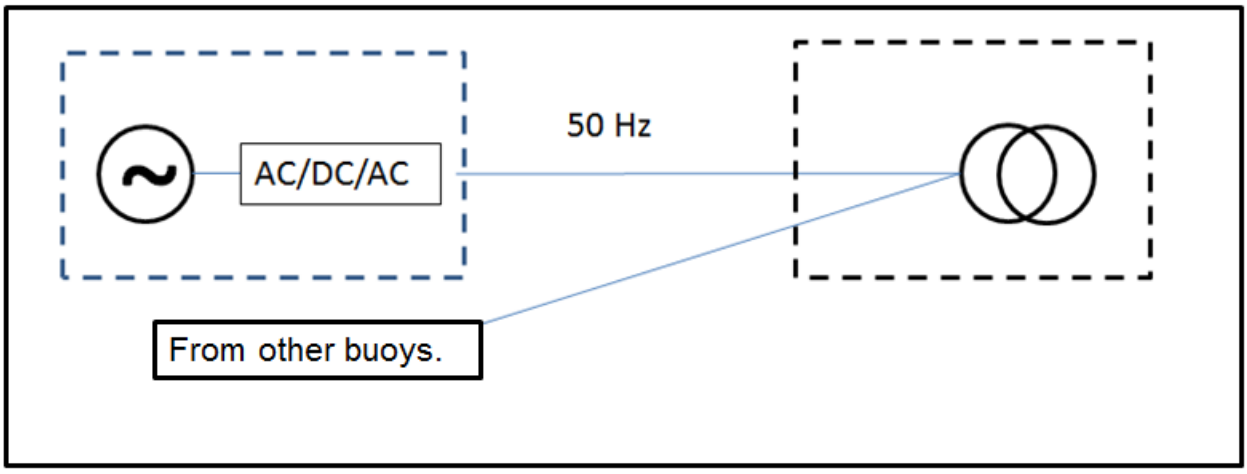

Figure 9: 50 Hz frequency link

2.3 Proposed system

The first topology with conversion stages of the buoys and transformer has a DC link. In this case the installation cost would be high. The losses will be notable and include the power losses in the converters and the DC link between the buoys and the floating transformer hub.

The second topology with the variable link is not suitable choice. The reason being the selection of the cables for each individual buoys. This could result in high cost. The AC-DC-AC converter on the floating transformer hub will have losses and would make the hub bulky hence the maintenance could be a concern.

The third topology with conversion stage on the buoy itself is a better choice. The reason is that 50 Hz AC signal is readily available at the buoys. This will enhance the system performance as auxiliary power is available and can be transported on the same connecting link. The system would have lower amount of components and hence the installation cost would decrease. The losses in the system would be lower as compared to the previous topologies. Hence the system with the 50 Hz link between the buoys and the floating transformer hub will be considered further.

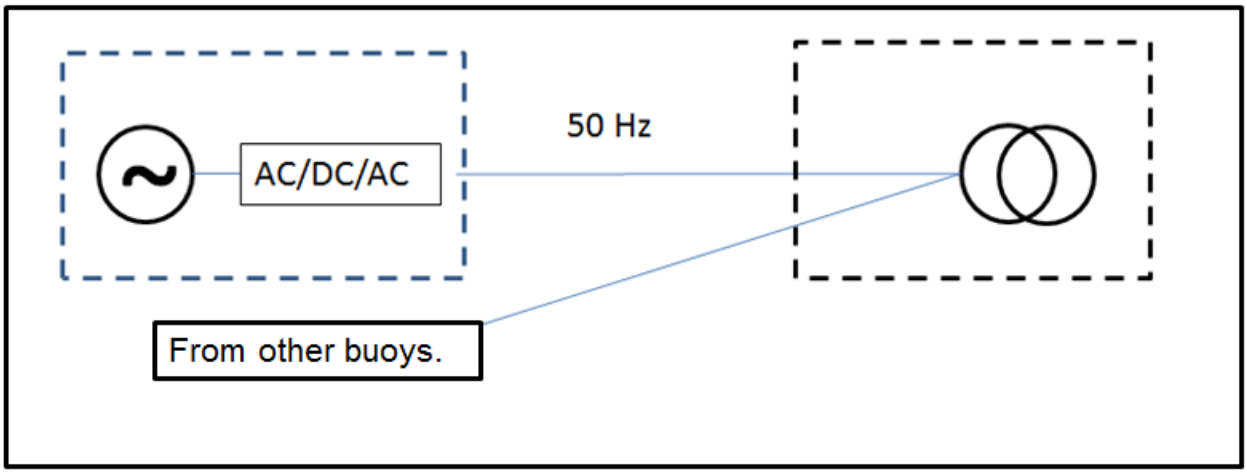

Figure 10: Proposed system for the transmission

The system comprises of an electrical generator with a frequency converter to convert the frequency to 50 Hz. A cable, couple of hundred meters long, to connect the buoys with the floating transformer hub. Here it is important to note that as there are several buoys connected together in a wavefarm. The other buoys would look exactly the same having similar components and then connected to the floating transformer hub.

3. Electrical Generator

An electrical generator is a device which converts the mechanical energy into electrical energy. In the case of Wave El buoy, hydraulic motor is coupled with the electrical system. Maximum power output from the electrical generator is 30 kW and the voltage level is 0.4 kV. Keep in consideration the constraints; an electrical generator is requisite that can efficiently convert the energy from the waves into electrical energy. Some of the conversion schemes are given below

3.1 Conversion schemes

There are two types of conversion schemes for the wave energy. One of them is the electrical conversion and the other one is the hydraulic conversion.

3.1.1 Electrical Conversion

In this type of conversion, an electrical device is used to convert the heaving motion of the waves into electrical energy. This can be seen in the figure below

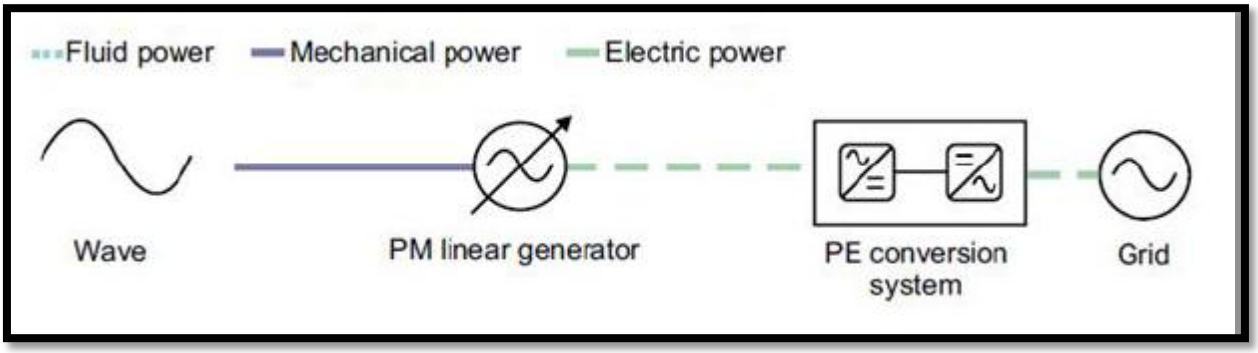

Figure 11: Electrical Conversion [7]

In the figure above a permanent magnet (PM) linear generator is being used. With the heaving motion of the wave, the linear generator moves vertically. A linear generator consists of insulated conductor, NdFeB permanent magnet and steel of different quality. The EMF is induced with the vertical motion of the piston caused by the waves. A floating buoy is connected with the piston which is surrounded by electric coils. The piston is anchored to the sea bed. The whole setup containing the linear generator is made water tight using a water proof container to withstand the severe environment of the sea.

3.1.2 Hydraulic conversion

In this type of scheme, hydraulic pump is coupled with an electrical generator to produce the electrical energy. The hydraulic system rotates with the motion of the waves and in turn rotates the electrical generator coupled to it. This can be seen in the figure below:

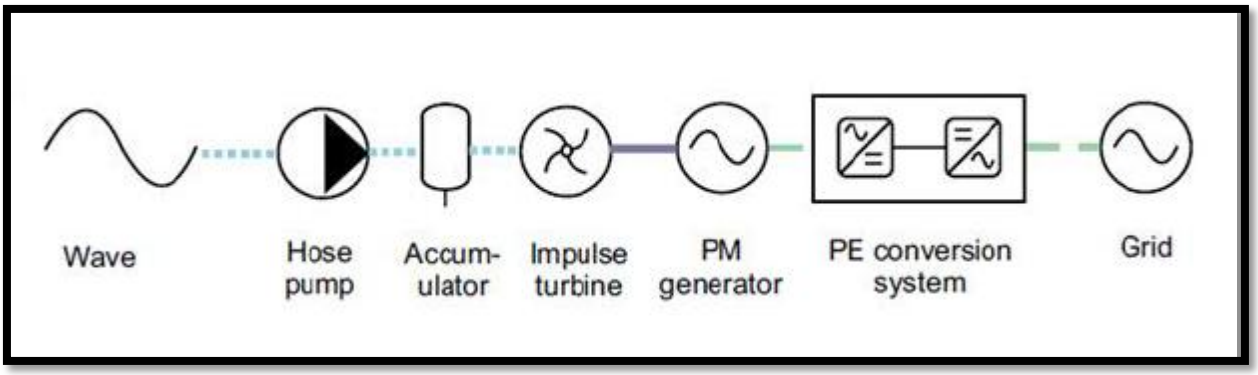

Figure 12: Hydraulic Conversion [7].

Hose pump is a positive displacement pump used to pump water into the accumulator. An accumulator is a pressure storage device. It is used to store the fluid under pressure by an external source. This is coupled to an impulse turbine which is coupled to the shaft of the electric generator. The wave motion enforces the hose pump to pump water into the accumulator where the pressure is maintained, than the water rotates the impulse turbine coupled to the shaft of the electrical generator to produce EMF. The produced EMF has a variable frequency and variable amplitude. In the figure a PM generator is used. It is worthy to note here that any generator can be employed to produce electrical energy.

3.1.3 Wave El Buoy conversion scheme

Wave El Buoy employs hydraulic conversion scheme. Hydraulic motor is coupled with the electrical generator. This can be observed in the figure below

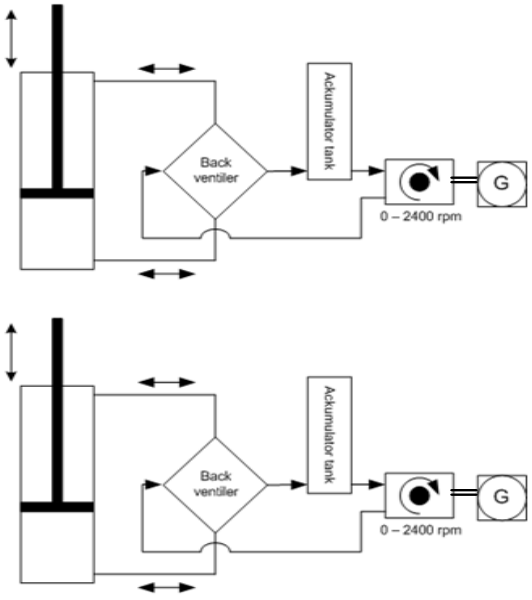

Figure 13: Wave El Buoy Conversion Scheme

3.2 Electrical Generator Options

There are several generator options that can be employed to extract electrical power from the waves. It is important to note that in this project the hydraulic conversion scheme will be used. There are many generator types used for the power conversion nowadays e.g. wound rotor synchronous generators, induction generators, PM synchronous generators etc. These generator types will be briefly discussed

3.2.1 Synchronous generator

Synchronous generators are commonly used to convert the mechanical power output from steam turbines, gas turbines, hydro turbines into electrical energy for the grid. These can be very large and reach the power rating up to 1500 MW. The name synchronous generator depicts that they operate at a synchronous speed. This means that the speed of rotor always matches the speed of the supply frequency. There are two main types into which a synchronous generator can be classified

3.2.1.1 Wound rotor synchronous generator

In this type of synchronous generator the DC field is supplied through the slip rings which are connected to the rotor. It has a stationary armature with 3-phase winding on the stator. DC supply is normally produced by the DC generator mounted on the same shaft as that of the rotor.

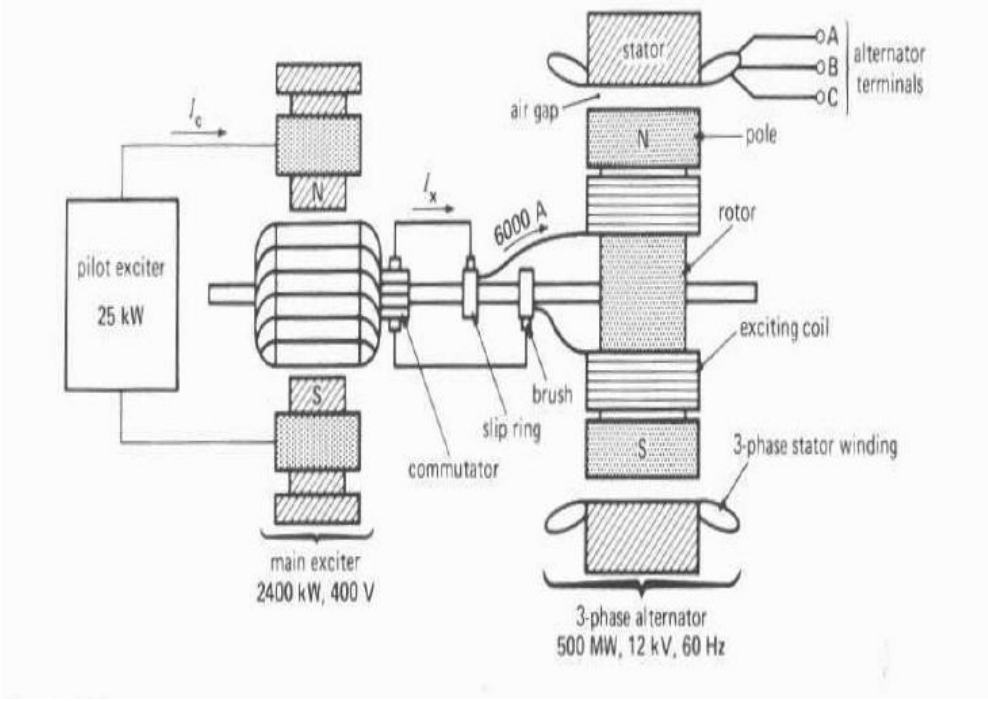

Figure 14: Wound rotor synchronous generator with slip rings [8]

Figure 12 shows the WRSG with slip rings. The pilot exciter permits the variable field control of the main exciter. The main exciter produces the main field. This is mounted on the same shaft as that of the rotor. It is connected through the slip rings. Three phase winding is connected to the stator. The stator of the synchronous generator is similar to that of a 3-phase induction machine i-e, stator consist of a cylindrical laminated core containing slots carrying a 3-phase winding. The nominal line voltage of a synchronous generator depends upon the KVA ratings, the greater the power rating; the higher will be the voltage. The rotor can be one of the two types

- Salient-pole rotor
- Cylindrical rotor

The salient pole rotors are used for low speed applications which require a large number of poles to achieve required frequencies such as hydro turbines. The cylindrical rotors are used for high speed applications such as steam or gas turbines.

The slip rings offer maintenance issues. To cope with this problem power electronics is employed. A type called brushless excitation can be used. In this type of configuration there are no brushes/slip ring assemblies.

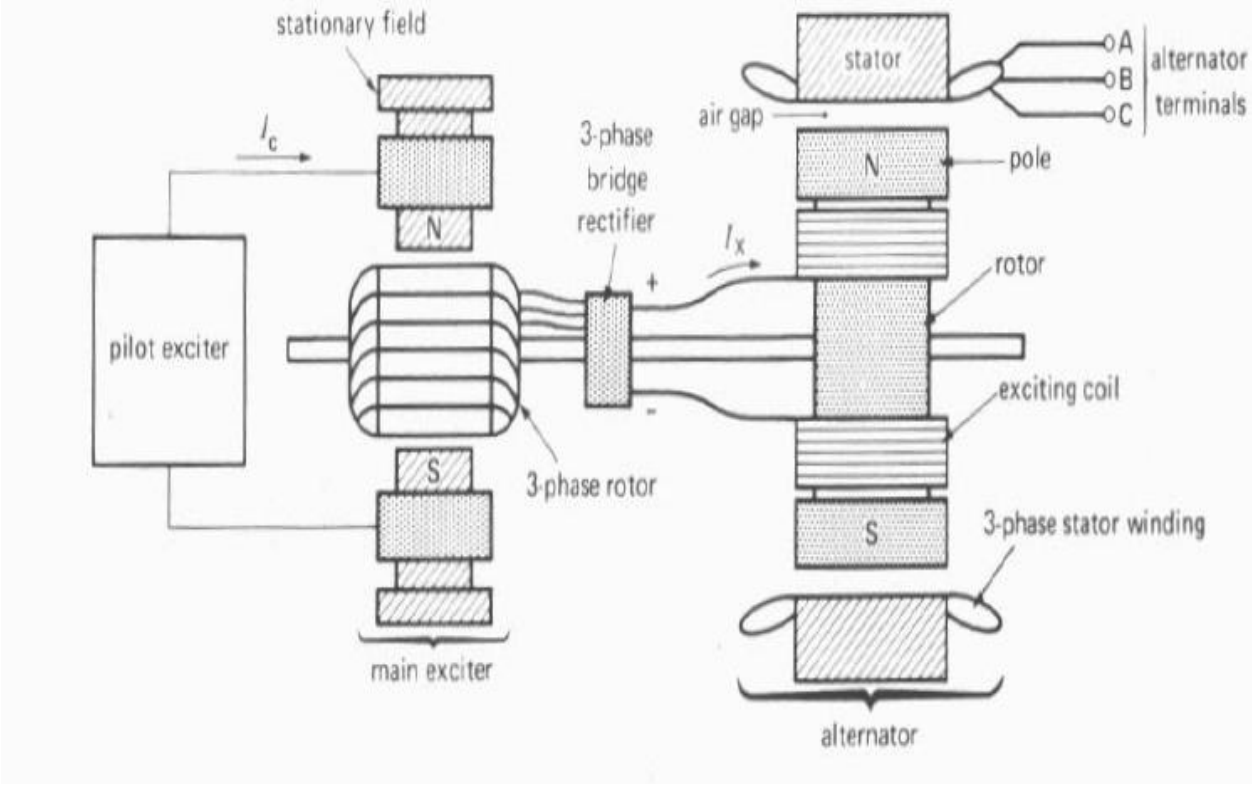

Figure 15: Brushless exciter system [8]

A typical brushless exciter system is shown in the system above. A 3-phase bridge rectifier is used to provide DC field to the rotor of the synchronous generator.

3.2.2 PM Synchronous Generator

In this type of synchronous generator, permanent magnets are placed within the rotor, hence there is no need of a DC exciter in this case. This means that the generator can self-magnetize. This kind of generator has a higher efficiency due to the fact that no energy is required to supply the field. The stator of a permanent magnet synchronous generator consists of three-phase winding similar to the one discussed in above types. The rotor consists of permanent magnets and the rotor type can be salient or cylindrical.

3.2.3 Induction Generator

Induction generator is asynchronous generator which works on the principle of the induction motors. The operation is that the rotor of the machine is made to turn faster than the synchronous speed producing negative slip. The induction generators are not self-magnetizing this means that they require an electrical supply to produce that rotating magnetic field. The rotating magnetic field from the stator induces current in the rotor of the generator. If the rotor rotates slower than the rate of the rotating magnetic field then the machine acts like an induction motor, but if the rotor rotates faster than the rotating magnetic field then the machine acts as a generator. Doubly fed induction generator is a type of induction generator that is used widely in the wind energy sector nowadays.

3.2.3.1 Doubly Fed Induction Generator

It is typically used for high power applications [9]. Doubly fed induction generator (DFIG) is a wound rotor machine where the rotor is connected to external variable voltage and frequency source using slip rings. The stator is connected to the grid network. Doubly fed induction generators were not so much popular in the past due to the maintenance requirements of the slip rings. Power converters usually cope with this problem for the variable frequency source for the rotor.

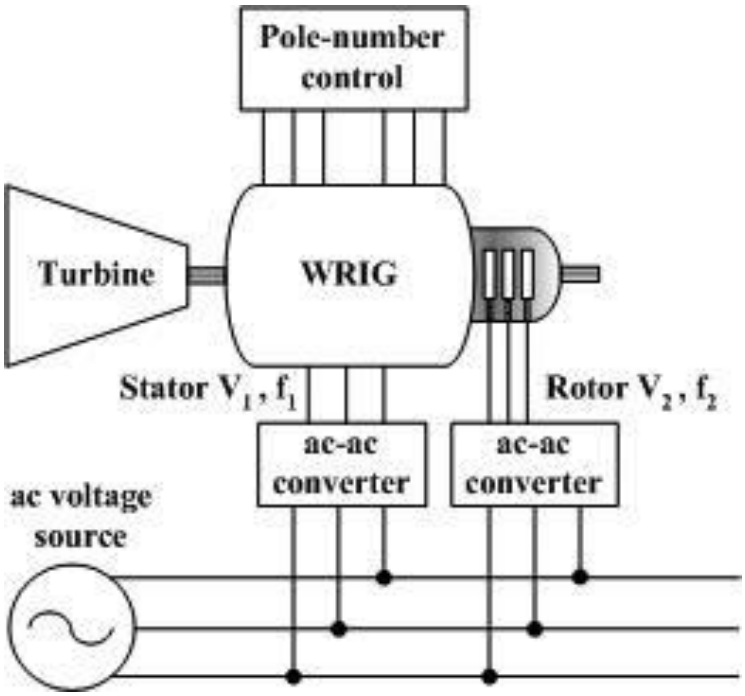

Figure 16: Doubly fed induction Generator [9].

3.2.4 Synchronous Reluctance Machine

The synchronous reluctance machine works on the concept of magnetic reluctance. In this type of machine the stator is identical to that of a typical induction or synchronous machine. A rotating magnetic field is produced by the sinusoidally distributed windings in the stator. The rotor is shaped with a small air gap in the direct (d) axis and a large gap in the quadrature (q) axis. The rotor is made of iron laminations separated by nonmagnetic material.

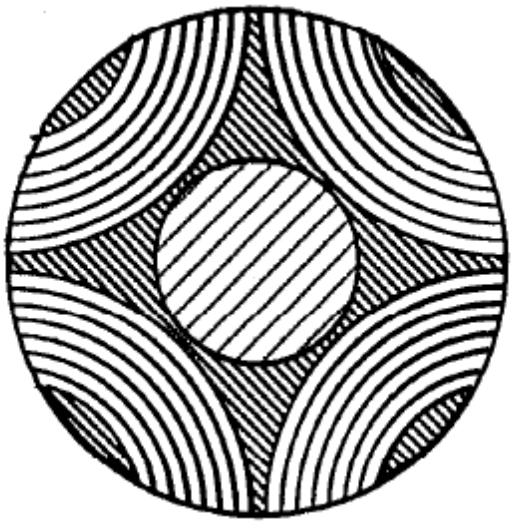

Figure 17: Axially laminated rotor for SyncRM [10].

3.3 Synchronous Reluctance Generator vs. Induction Generator

Synchronous reluctance machine is a new machine concept. Induction machines are being widely used in the industry nowadays. In the case of low power (i-e. 30 kW) application both machines are available and can be employed. A brief comparison is made between the two machines to inspect the effective and feasible solution.

The torque of an induction machine is given by following equation [11]

$$T_i = \frac{3}{2} p K_r \lambda_r i_{qi} \tag{3.1}$$

Where,

$p = No.\ of\ pole\ pairs.$

$K_r = char - coefficent\ depends\ upon\ relation\ between\ self\ and\ mutual\ inductances.$

$\lambda_r = rotor\ flux\ linkage.$

$i_{qi} = q - axis\ current.$

The torque of synchronous machine is given by [11]

$$T_{syncr} = \frac{3}{2} p\left(\lambda_d i_{qsy} - \lambda_q i_{dsy}\right) \tag{3.2}$$

Introducing the coefficient K_{dq} that depends upon the motor inductance

$$T_{syncr} = \frac{3}{2} p K_{dq} \lambda_d i_{qsy} \tag{3.3}$$

Let us assume the following relations [12]

$$R_{rot} = 0{,}8 * R_{stat} \tag{3.4}$$

$$K_r = 0{,}97 \tag{3.5}$$

$$\mathrm{K_{dq}} = 0{,}9 \tag{3.6}$$

$$\frac{i_d}{i_q} = 0{,}4 \tag{3.7}$$

As the induction machine and the synchronous reluctance machine have the same stator geometry. The relation between rotor and stator of the machines are stated as above. The machines analyzed for the comparisons have the same stator hence the two machines show nearly the same air gap flux density, the torques can be written as

$$T_i \propto K_r * i_{qi} \tag{3.8}$$

$$T_{syncr} \propto K_{dq} * i_{qsy} \tag{3.9}$$

Considering the above assumptions the comparison of the two machines at same torque and dissipated power will be carried out.

3.3.1 Machine comparison at the same torque

Here it can be noted that the induction machine and the synchronous reluctance machine are operating at the same torque

$$T_{sync} = T_i \tag{3.10}$$

This can be further simplified as

$$\frac{3}{2} p K_{dq} \lambda_d i_{qsy} = \frac{3}{2} p K_r \lambda_r i_{qi} \tag{3.11}$$

As a result it can be observed that the Synchronous reluctance machine requires a higher current then the induction motor. The relationship between the two motor currents is

$$i_{qi} = 0{,}93 i_{qsy} \tag{3.12}$$

It can be concluded that to produce the same torque the synchronous reluctance machine requires higher current then the induction machine. Here it is important to note that the higher currents are involved in both stator and rotor windings the joule losses are lesser in the synchronous reluctance machine. This can be seen in the following relations

$$\frac{P_{loss,i}}{P_{loss,sync}} = 1{,}53 \tag{3.13}$$

$$\frac{P_{loss,sync}}{P_{loss,i}} = 0{,}65 \tag{3.14}$$

3.3.2 Machine comparison at the same dissipated power

In this case we assume that both the machine is having the same dissipated power.

The losses in the windings of the two machines are given as

$$P_i = \frac{3}{2}\left[R_{stator}\left(i_{qi}^2 + i_{di}^2\right) + R_{rotor} i_{qrotor}^2\right] \tag{3.15}$$

$$P_{sync} = \frac{3}{2}\left[R_{stator}\left(i_{qi}^2 + i_{di}^2\right)\right] \tag{3.16}$$

Where

$R_{rotor} = Resistance\ of\ the\ rotor$

$R_{stator} = Resistance\ of\ the\ stator$

As the two machines have the same dissipated power hence

$$P_{loss,i} = P_{loss,syncr} \tag{3.17}$$

$$\frac{3}{2}\left[R_{stat}(i_{qi}^2 + i_{di}^2) + R_{rot} i_{drot}^2\right] = \frac{3}{2}\left[R_{stat}(i_{qsy}^2 + i_{dsy}^2)\right] \tag{3.18}$$

By using the parameters of the synchronous reluctance and the induction machine it can be seen that

$$i_{qi} = 0{,}78 i_{qsy} \tag{3.19}$$

With the above current relation the torque of the machines can be computed as

$$\frac{T_i}{T_{sync}} = 0{,}84 \rightarrow \frac{T_{sync}}{T_i} = 1{,}19 \tag{3.20}$$

It can be concluded that with the same dissipated power the synchronous reluctance machine is capable of producing better torque then the induction machine.

3.4 CONCLUSION

The above comparison between the induction machine and the synchronous reluctance machine depicts that the synchronous reluctance machine requires higher current then the induction machine of the similar rating at equal torque but the power losses are lower in the syn-

chronous reluctance machine. Hence the induction machine is more hot then the synchronous reluctance machine. At the same dissipated power the synchronous reluctance machine is capable of producing higher torque then the induction machine. Hence it can be concluded that the synchronous reluctance machine can be a viable alternative machine for the power production in the wave energy converter.

4. Frequency Converter

The frequency converter or power electronic converter plays a vital role in the efficient and economical power transfer from the buoy to the floating hub. There are several connection topologies discussed in the earlier chapter in which the frequency converter can be employed either both at the WEC and the floating hub. A Single converter can be connected at the output of the generator and then the power can be transported or the same converter can be placed on the floating hub instead. As observed in the earlier discussion that the power transportation scheme to be employed will be a 50 Hz AC link from each buoy to the input of the floating hub, hence a frequency converter must be employed that rectifies the variable AC frequency to DC, than inverting the DC back to 50 Hz AC. This 50 Hz AC signal can then be fed to the input of the floating transformer.

4.1 Frequency Converter Selection

Selection of the frequency converter depends upon the topology used, the frequency converter techniques and the power electronic converter employed to convert the signal to a suitable frequency level. Thyristor is the semiconductor device that was used in late 1950s. With growing power demand and research, development of power electronic devices cannot be neglected. At present age there are several devices that can be used for high power and high frequency applications. A brief description of the semiconductor devices is given as follows

4.1.1 Diodes

Diode is a device consisting of semiconductor material. Ideally a diode behaves as a short circuit, if the polarity of the voltage across it is positive. Diode can be visualized as a simple pn-junction with holes as majority charge carriers in p-type material and electrons and majority charge carriers in n-type material. On the other hand the diode behaves as open circuit, if the polarity of the voltage across it is negative. The first case is named as forward bias and the second case is named as reversed biased. The real behavior of the diode is somewhat different as that mentioned ideally. A small amount of voltage is needed in forward biased condition to allow the conduction through the diode. This voltage required persists as a voltage drop across the diode during the conduction. There is a maximum reverse voltage or breakdown voltage that needs to be avoided to protect the diode from damage. The ideal V-I characteristics and the real V-I characteristics can be seen in the following figure.

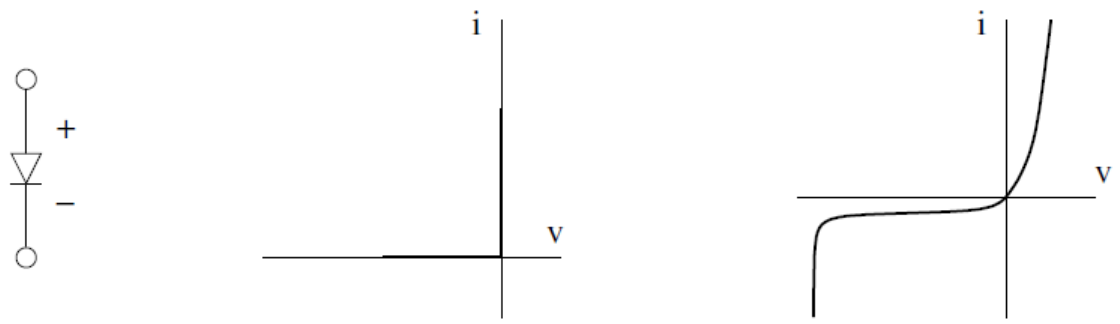

Figure 18: Diode symbol, Ideal and real V-I Characteristics

The symbol of the diode shows that the device can only conduct in forward bias. In reverse bias, if the voltage exceeds the breakdown voltage of the diode then the diode will damage.

There are different types of diodes depending upon the application [13]

4.1.1.1 Rectifier Diodes

In rectification applications the diodes are used to convert AC power to DC power.

4.1.1.2 Switching Diodes

In lower power applications switching diodes are used. These diodes function better on high frequencies

4.1.1.3 Zener Diodes

In power protection applications, Zener diodes are used. These diodes have an ability to recover from the reverse voltage if the breakdown voltage of the diode is exceeded.

4.1.1.4 Optical Diodes

In photo activated devices optical diodes are used. These diodes conduct when light is exposed on the surface.

4.1.1.5 Special Diodes

Other diodes such as Schottky diodes, varactors and tunnel diodes are used for the special applications

The diodes have an advantage of having lower cost than the other available alternatives. The construction of a diode is relatively simpler. The disadvantage of the diodes is that these devices only allow unidirectional flow of the current. The diodes also generate harmonic currents in the system which causes stability problems in the system.

4.1.2 Thyristors

We saw in the case of diodes that they are not controllable. Thyristor on the contrary is a semiconductor device that can be controlled. The Thyristor has a capability to be operated in various conditions. It can act as a switch, a rectifier which rectifies AC to DC or it can be used as a voltage regulator. The name Thyristor constitutes of two words, ´thyratron´ and ´transistor´. Thyratron refers to the analogue of thyratron vacuum tube and transistor refers to its resemblances with the transistor.

The Thyristor consist of three electrodes namely, gate, anode and the cathode. The anode and the cathode have the same working as we saw in the diode. The gate is the controlling electrode. The gate allows the flow of current from anode to cathode once a small current is injected into it. The Thyristor consist of four semiconducting layers. These are the same P type and N type layers used in the case of the diodes. In the case of Thyristors the layers are alternative (PNPN). The Thyristor continue to conduct unless the voltage across it is not reversed.

4.1.2.1 Silicon Controlled Rectifier

Silicon controlled rectifier (SCR) is a type of thyristor. When the cathode of SCR is negatively charged and anode is positively charged, no current flows through the device until a gate pulse is applied to the gate terminal. The conduction stops when the voltage is reversed or decreased below a certain threshold. This triggering pulse applied on the gate terminal allows controlling or switching large powers in the system.

4.1.3 Insulated Gate Bipolar Transistor (IGBT)

Insulated gate bipolar transistor often called IGBT is used to take the advantage of both metal oxide semiconductor field emitting transistor (MOSFET) and bipolar junction transistor (BJT). IGBT has wide range applications such as in power electronics, power system and telecommunication.

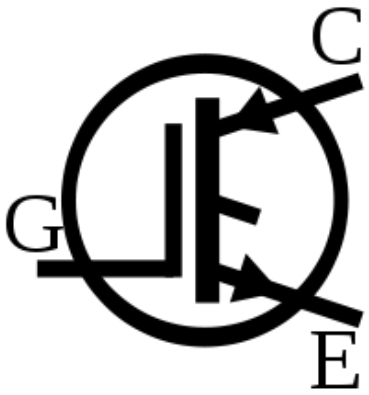

Figure 19: Circuit symbol of an IGBT

Figure 17 shows the circuit symbol of an IGBT. It has three terminals namely collector (C), gate (G) and emitter (E).

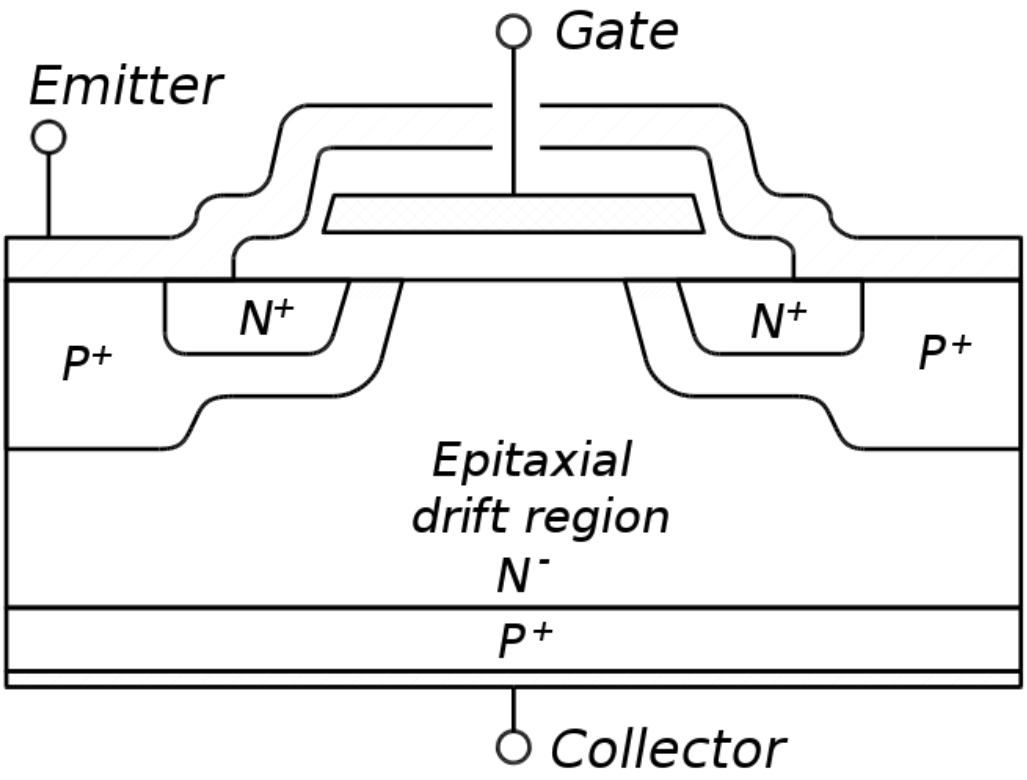

Figure 20: cross section of an IGBT cell

Figure 18 shows the cross section view of a single IGBT cell. The P^+ layer at the bottom of the cell can either work as a drain or a collector. The N^+ layer at the top acts as a source.

The IGBTs have many advantages over other semiconductor devices such as MOSFETs, JFETs and BJTs [14].

- IGBT is much cheaper than counter parts. The reason is that it has very low on-state voltage drop and the on-state current density is very high.
- It is possible to have a smaller chip size.
- IGBT has simple control technique as compared to other current controlled devices such as thyristors and BJTs in high power applications.
- It is safer to use IGBTs due to its better current and voltage handling capabilities.
- Unlike thyristors, IGBTs can be switched on and off at arbitrary time instant.

4.1.4 Silicon Carbide Based Insulated Bipolar Transistor (SiC IGBT)

Silicon carbide based devices are very recent in the market nowadays. The research in SiC based devices has proven various advantages over the other semiconducting devices for switching and high power applications [15]. The Silicon Carbide is a better option because it has a wide range of advantages on the other similar material. This device has a wide range of operating voltage about 1000 V. with SiC it is possible to have low leakage currents as the semiconductor barrier is larger than that of silicon. It has higher breakdown field strength hence larger on-resistance. SiC has higher current densities and thermal conductivity [16]. With all these advantages SiC devices are limited to applications such as switch-mode power supplies and power factor correction [17]. The reason for these limited applications is the high SiC market price.

4.2 ABB´s Frequency converter modules

The eventual choice became the ABB´s ACS850-04 and ACSM1-204 frequency converters. These modules are compatible with the desired power level for the WECs i-e, 30 kW. These have a very attractive modular structure and can be employed with any electrical generator. A brief description of the described frequency converters is given below

4.2.1 ACS850-04 Frequency Converter

The ACS850-04 module is frequency converter manufactured by ABB. The modular structure can be seen below

Figure 21: ACS850-04 Module [4]

The circuit diagram of the module is in the figure below

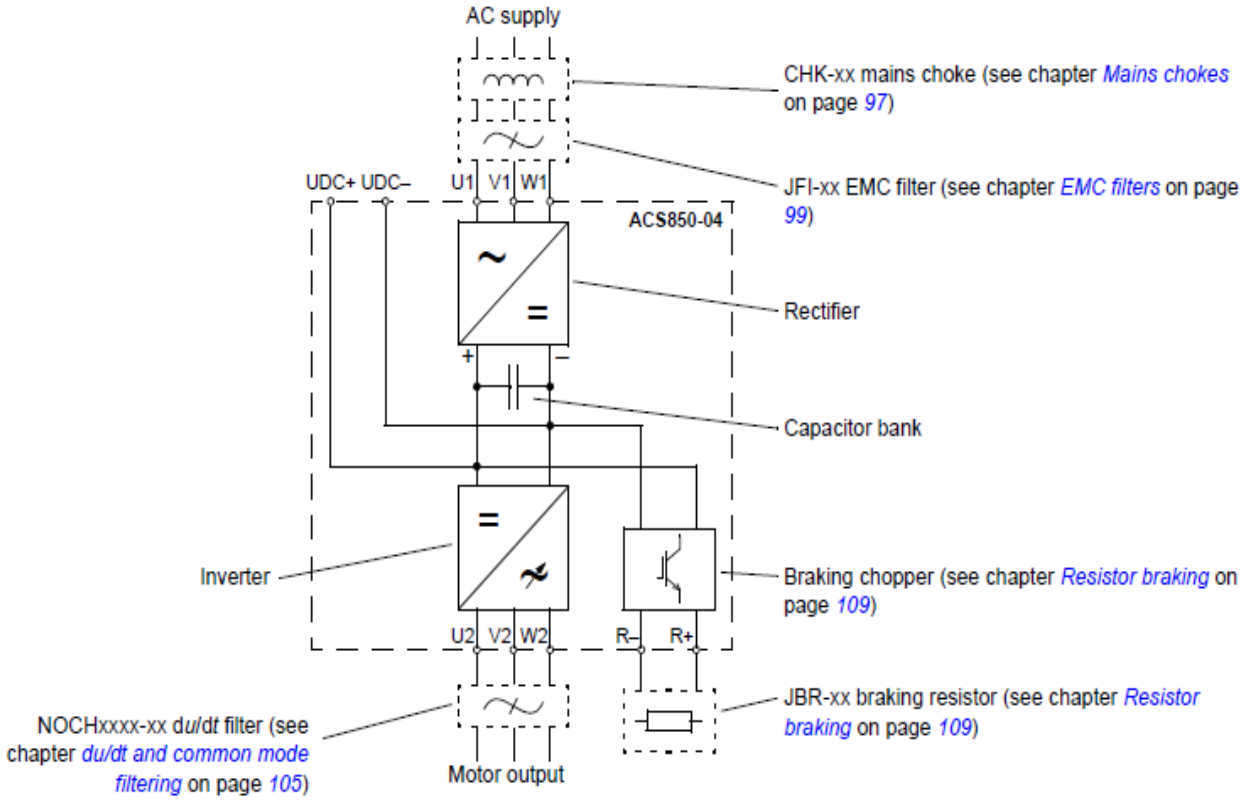

Figure 22: ACS850-04 Main circuit [4]

In the above figure we can see the main components of the module [4]

4.2.1.1 Braking chopper

The braking chopper is built in component of the module. It conducts the energy generated for example from a decelerating motor to the braking resistor.

4.2.1.2 Braking resistor

The braking resistor is an external component and is not built in the module. It dissipates the energy fed from the braking chopper and converts it into heat.

4.2.1.3 Capacitor bank

Capacitor bank is used for the energy storage and provides stability to the system.

4.2.1.4 Inverter

DC is converted to AC and vice versa by the IGBT based inverter.

4.2.1.5 Mains Choke

The mains choke reduces the harmonics in the input current and reduces disturbances and low frequency interference in the supply.

4.2.1.6 EMC Filter

Electromagnetic compatibility (EMC) filter consists of choke, capacitor and resistor. It provides protection to the system from the noise and electric fields.

4.2.1.7 Rectifier

The rectifier rectifies the AC voltage to DC voltage. The module consists of diode rectifier [4].

ACS850-04 module is an attractive and feasible choice as a frequency converter, but the problem lies with the rectifier part. It consists of diodes and controllability is the concern with this type of rectifier. As mentioned in the previous section that the diode rectifier offers unidirectional flow of the current hence the system stability is a concern when these rectifiers are employed. In order to cope with this problem another module ACSM1-204 is employed which has the similar circuitry as the ACS850-04 module but in this case both the IGBT inverters from each module will be used at input and the output.

4.2.2 ACSM1-204 Frequency Converter

As discussed in the previous clause, ACS850-04 module consists of diode rectifier which limits the controllability of the power. In order to cope with this problem another module is employed. ACSM1-204 is another frequency rectifier manufactured by ABB.

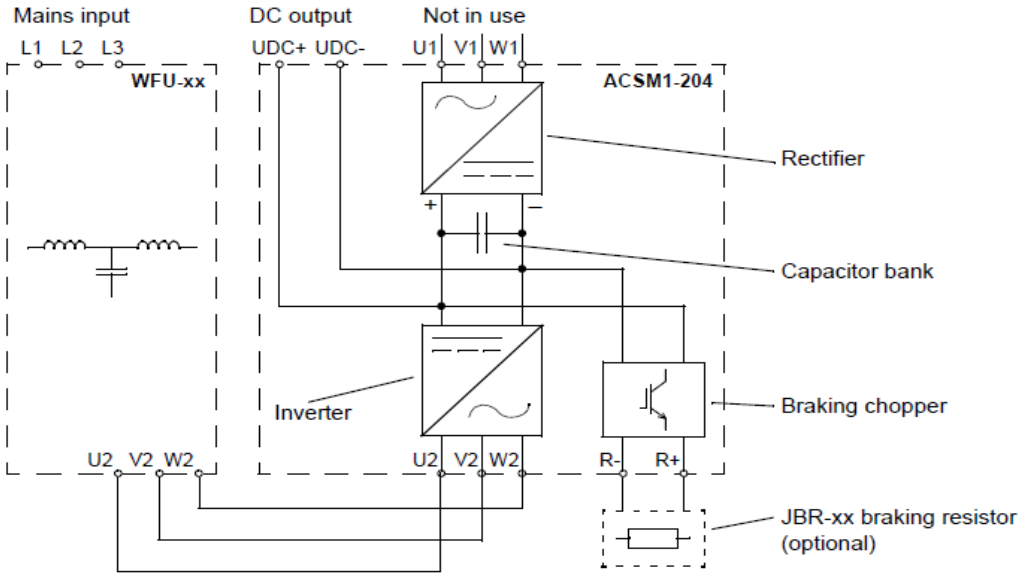

Figure 23: ACSM1-204 Main Circuit [3]

The main circuit of ACSM1-204 is shown in figure 17. The circuit shows that he components resembles to that of ACS850-04. In ACSM1-204, diode based rectifier is used. Hence a bypass methodology can be used to connect the IGBT inverters of the two modules namely ACS850-04 and ASM1-204. This can be done by simple wiring alteration. This will be discussed in next section. The ACSM1-204 has similar architecture as that of ACS850-04. The inverter is IGBT based and a braking chopper and braking resistor is available for the dissipation of the energy. Braking resistor is however optional component which can be neglected, as in the case of coupling ACSM1-204 with ACS805-04, one of the braking resistor can be used [3].

In figure 21, mains input module is shown. This module has filter that smooths the line current waveform that may contain disturbance. This device filters all the harmonics and ripples on the switching frequencies.

4.3 Main circuit with ACS850-04 and ACSM1-204

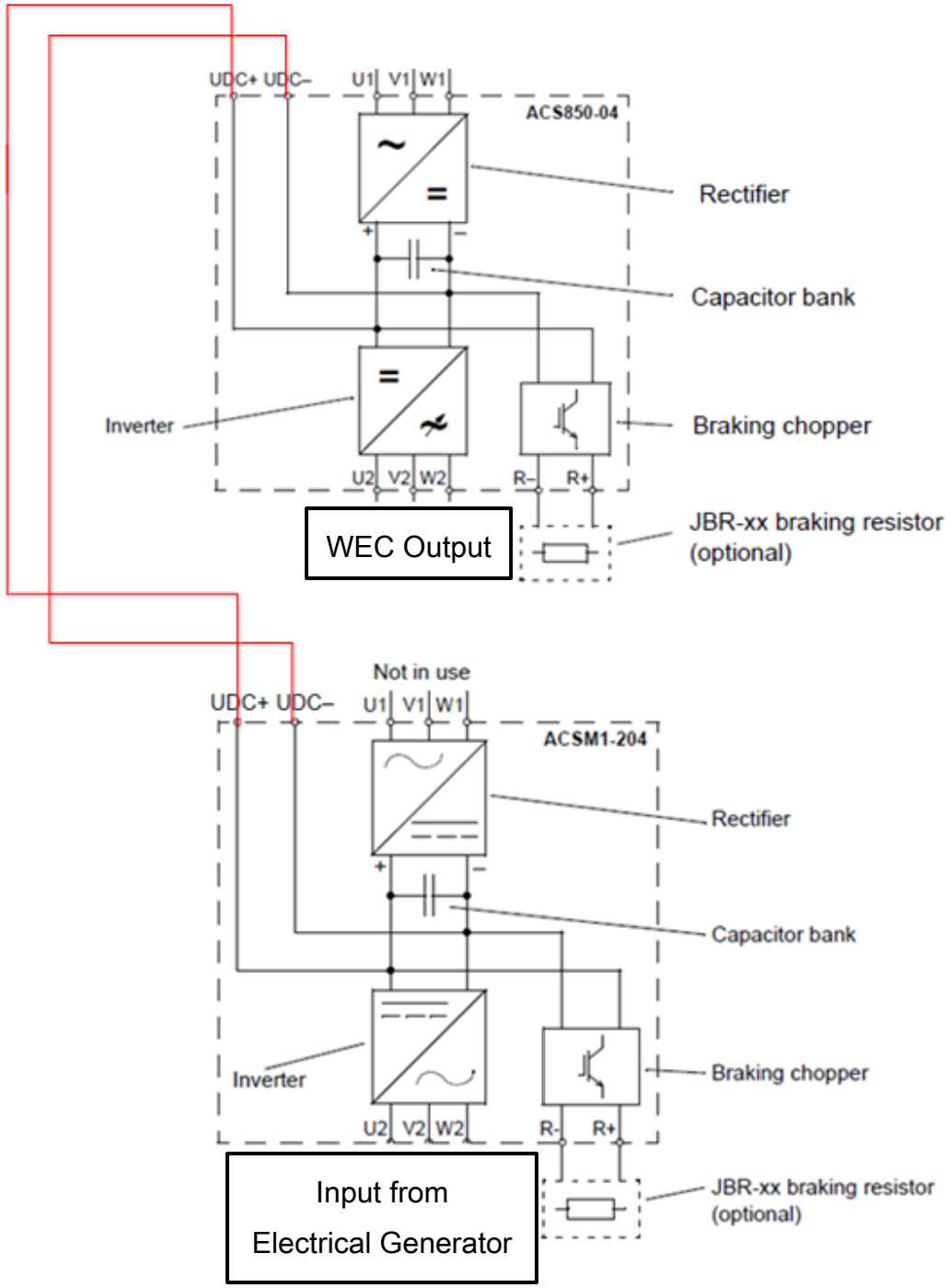

Figure 24: Main circuit with ACS850-04 and ACSM1-204 [4] [3].

Figure 22 shows the main circuit comprising of ABB´s ACS850-04 and ACSM1-204 frequency converter modules. For the sake of simplification it can be observed in the above picture that some of the details are not shown in the schematic. The power input is fed into ACSM1-204

from the hydraulics. This signal is low voltage and consists of variable frequencies. The input is given to the IGBT Inverter which in this case acts like a rectifier and converts the variable frequency signal to DC. This DC signal is then fed to ACS850-04 and converted back to AC by IGBT inverter. The frequency of the signal is 50 Hz as required to transmit to the floating transformer.

4.4 Conclusion

It can be concluded from the above discussion that ABB´s modular frequency converters can offer various advantages as compared to its counter parts. The devices namely ACS850-04 and ACSM1-204 have compact modular structure. It is convenient to mount these devices within the wave energy converter. Employing ACSM1-204 with ACS850-04 enhances the control capability of the power flow. The power ratings of these devices suits well with the 30 kW application of wave EL Buoy. Moreover the braking chopper and the braking resistor provide effective stability for the power flow. The storage unit or the capacitor bank provides better stability to the system in case of a fault or voltage sag.

On the other hand ACS800 drive module manufactured by ABB consists of two IGBT stages, one for the rectification and other for the inversion. This module is expansive as compared to the combined cost of the two prescribed modules. Hence ACS850-04 and ACSM1-204 are economical and feasible options for the frequency converter.

5. WEC Interconnection and Cabling

ABB´s Synchronous reluctance generator and IGBT based frequency converter are efficient solution for electrical conversion from the mechanical input as discussed in the previous section. Hence the single wave energy unit can be visualized from the following figure

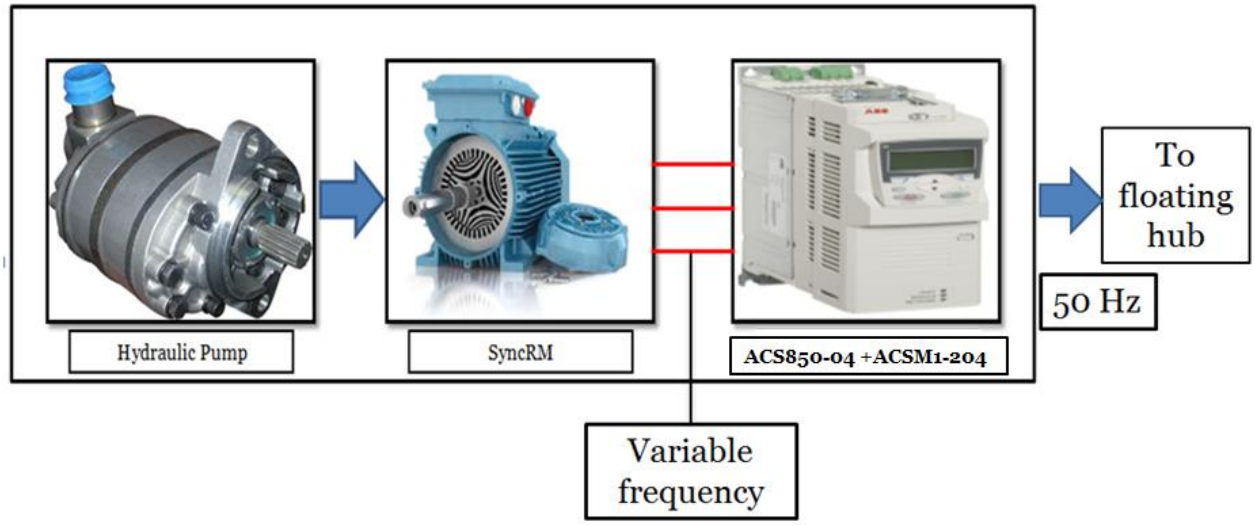

Figure 25: WEC structure with generator and frequency converter

It can be observed from the above figure that 50 Hz signal is the output from the WEC as desired. The hydraulic pump converts the potential and kinetic energy in the waves to mechanical energy. The pump is coupled with the synchronous reluctance generator and hence the mechanical energy is converted to electrical energy. The output from the synchronous reluctance generator is raw and contains variable frequency. It is required to change this frequency to a standard value to facilitate the control and transmission of the electrical power. ACS850-04 and ASM1-204 change the frequency of the output signal from synchronous reluctance generator to 50 Hz.

Scheme shown in figure 23 is a basic building block and can deliver a maximum power of 30 kW. It is important to interconnect these WECs effectively in a way to get optimum and economical transfer of power to the floating transformer hub. Many interconnection schemes have been developed and studied in recent past to interconnect the WECs. The bases of these interconnection schemes are

- Effectively transfer electric power with minimum power losses.
- Reduce the voltage drop.
- Reduce the total cost of the cables and connecting devices.
- Ensure the availability of the WECs to the floating hub and thereafter to the grid.

5.1. Interconnection Schemes

There are various configurations which can be adopted to achieve effective and economic power transfer from a set of WECs. A brief description of these configurations is given below

5.1.1. Single cable connection to the hub

In this type of scheme a single cable link connects the WEC to the floating transformer hub. This can be visualized in the figure below

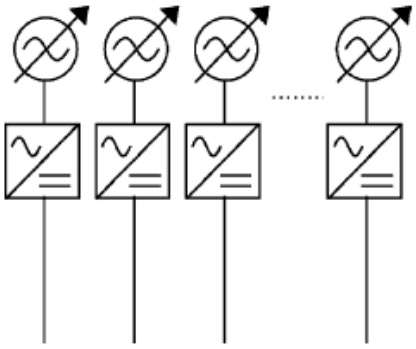

Figure 26: Single cable connection to hub [18]

This scheme has high availability of each WEC and simple design as advantages. High installation cost is a disadvantage.

5.1.2. Cluster scheme

In this type of scheme many WECs are connected together and forming a cluster. These clusters can be connected to the floating hub with one cable. In this case the cable connecting the cluster to the floating transformer hub must be rated to withstand the power generated by the cluster. The cluster scheme can be seen below

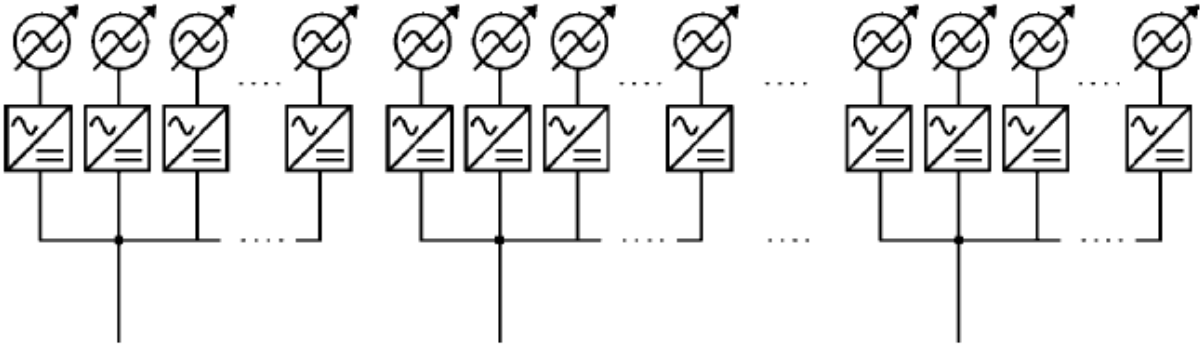

Figure 27: Cluster Scheme [18]

This scheme offer high availability but the interconnection and the placement of WECs within the clusters are complicated [18].

5.1.3. Subcluster and cluster Scheme

In this type of scheme the previously discussed clusters can be connected together and to the floating transformer hub with one cable. As mentioned previously the cable connecting several clusters and the floating transformer hub must be rated to withstand the power delivered by the clusters. This scheme can be observed below

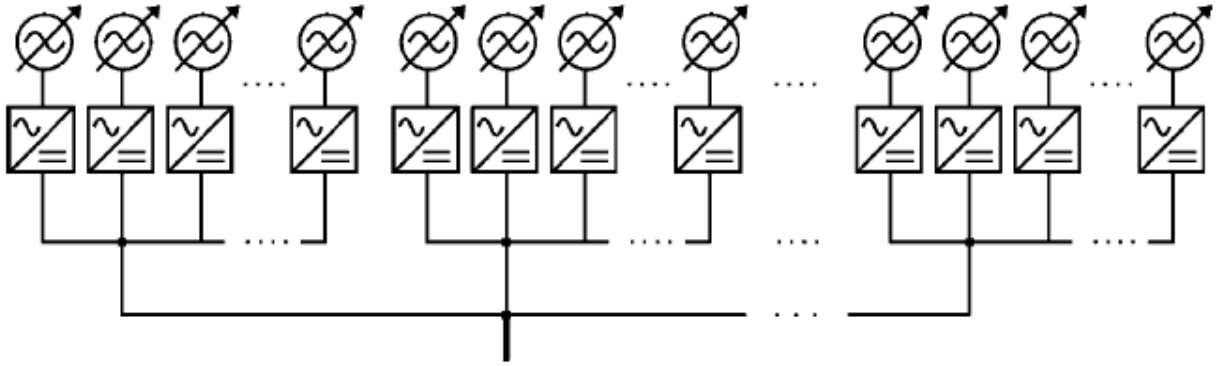

Figure 28: Subcluster and cluster scheme [18]

In the above scheme the installation cost is comparatively lower than the cluster scheme. Protection of the system is a concern if this scheme is adopted [18].

5.1.4. Radial Schemes

Radial scheme for the interconnection of WECs is employed in order to reduce the cable length and hence reduce the cable cost. The radial system offers better efficiency and reliability with reduced power losses and voltage drop per radial [19]. Figure below shows the radial scheme that can be employed for WEC interconnection.

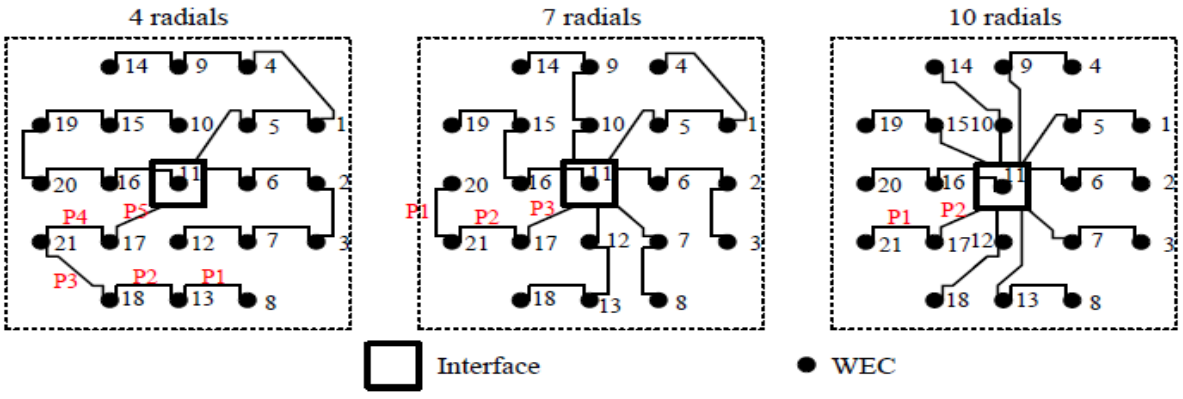

Figure 29: Radial scheme with 21 WECs [19]

Figure 27 shows radial 4, 7 and 10 radial schemes with 21 WECs forming each radial structure. Here it is important to note that P1 between the links means that the cable carries power output of one WEC. Similarly P2, P3, P4, P5 means that the cable respective cable links carry power

produced from 2, 3, 4 and 5 WECs. The interface shown in black square represents the floating transformer hub or the point of connection of all individual radials.

Another example of the interconnection schemes can consist of fewer WEC as compared to the previously discussed case. It can be observed in the figure below

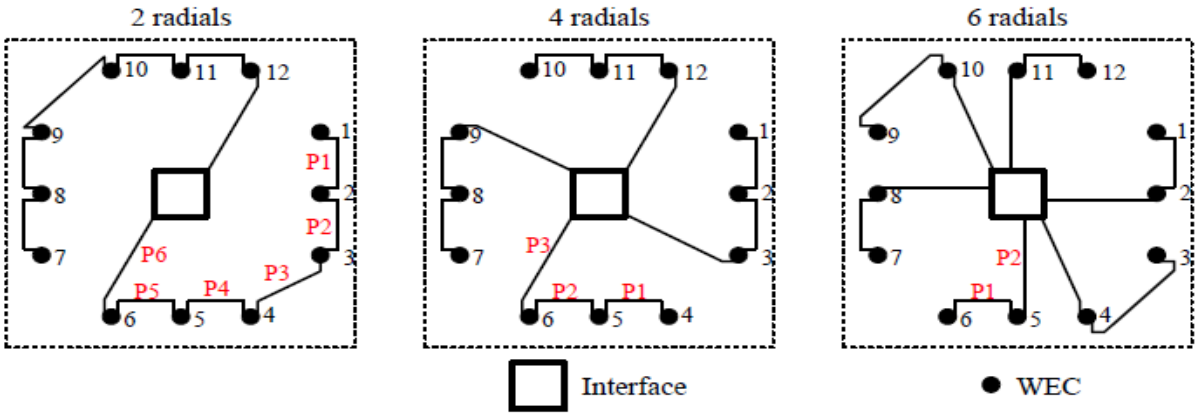

Figure 30: Radial scheme with 12 WECs [19]

The radial scheme shown above is the same as the previous one with less number of WECs connected in the radials.

5.2. Selected Scheme and System Definition

It can be seen from the previous discussion that the radial scheme has a tendency to be a better option for the interconnection of the WECs. Radial scheme discussed in the clause 5.1.4 will be adopted and analyzed for our designed system.

The system is characterized as follows

- 12 WEC´s connected to the floating hub.
- 30 KW maximum power output.
- 400V (231V) voltage level.
- 30 m distance between the WECs.
- Cable length (120m) per link.

The system attributes can be visualized from the following figure

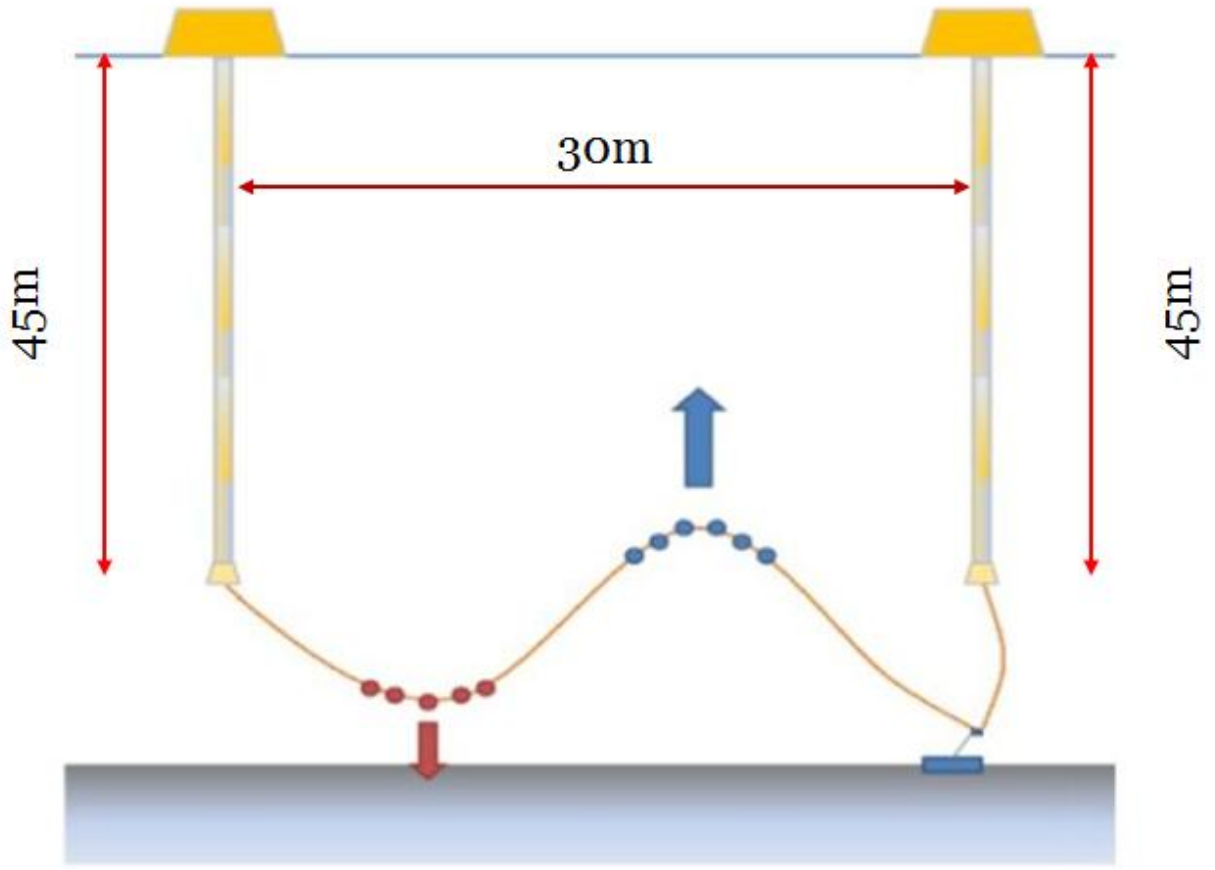

Figure 31: Distance between two WECs and the tentative cable length

The acceleration tube inside the water is 20m in length. Heaving cushion and the safety margin of 25m is given and hence the cable length from the generator to the bottom will be 45m. The distance between two WECs is approximately 30m and hence this would add in the total cable length. Collectively the cable length between two WECs would be 120m.

In order to find the most effective and economically sustainable radial scheme, various radial schemes will be analyzed, which are listed below

- 2 Radial scheme
- 4 Radial scheme
- 6 Radial scheme
- 12 Connections to the floating hub

Fig 32, 33, 34 and 35 represents the various radials schemes

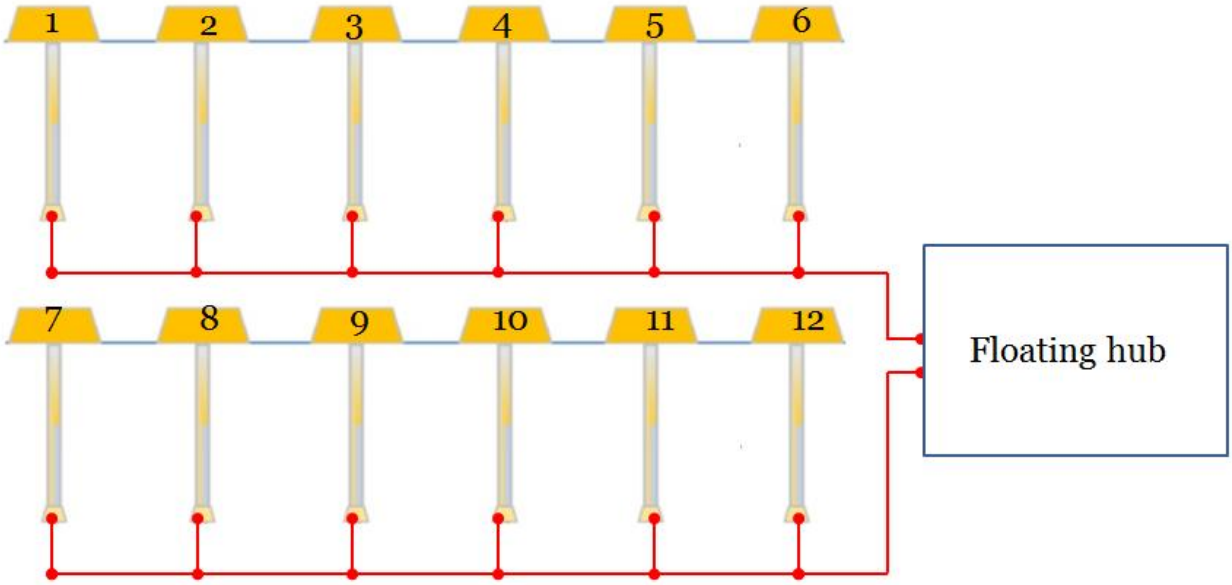

Figure 32: 2-Radial scheme

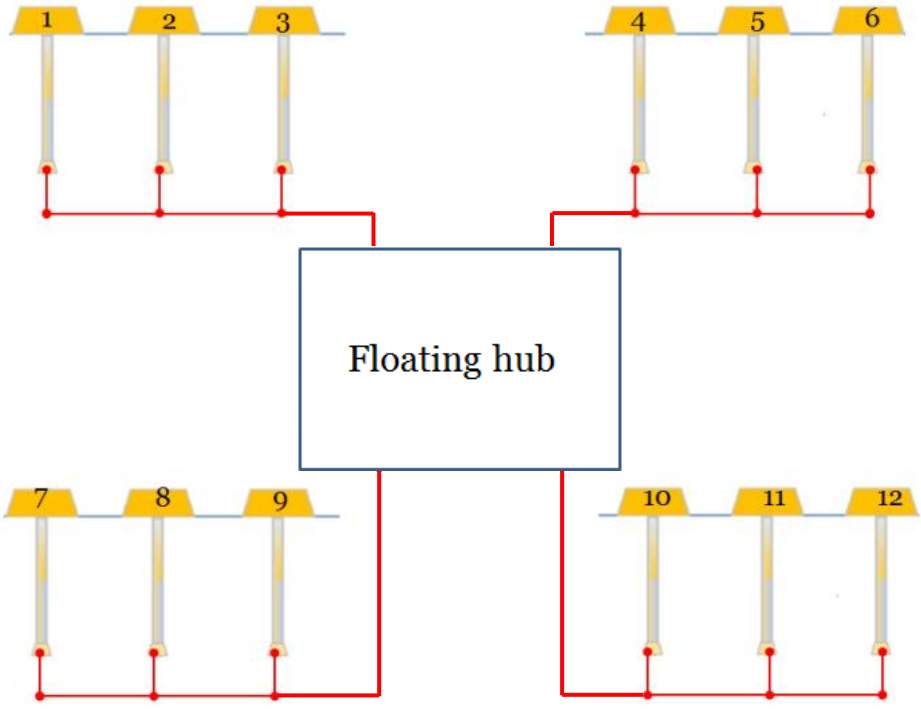

Figure 33: 4-Radial scheme

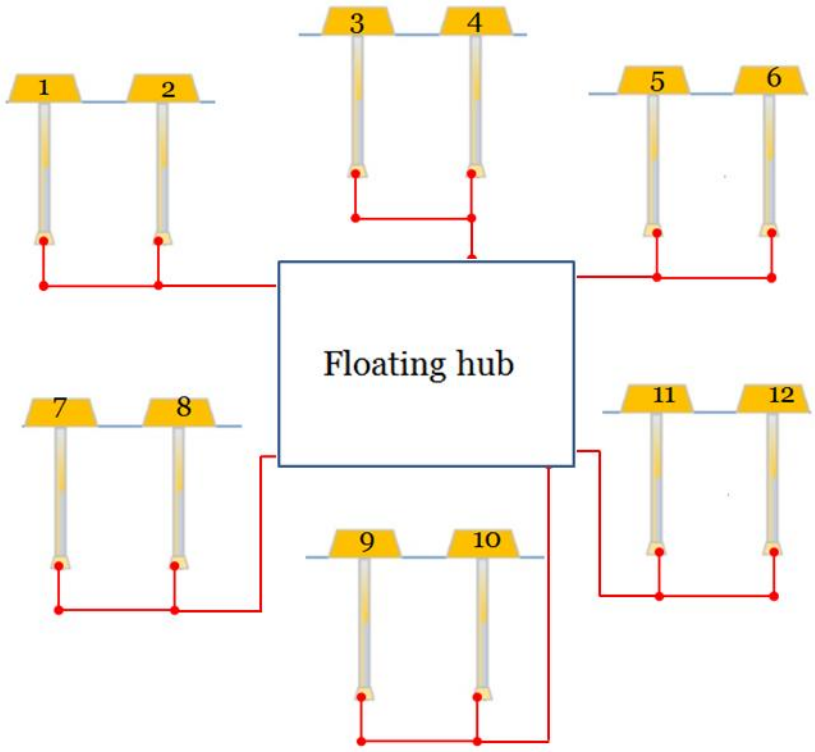

Figure 34: 6-Radial scheme

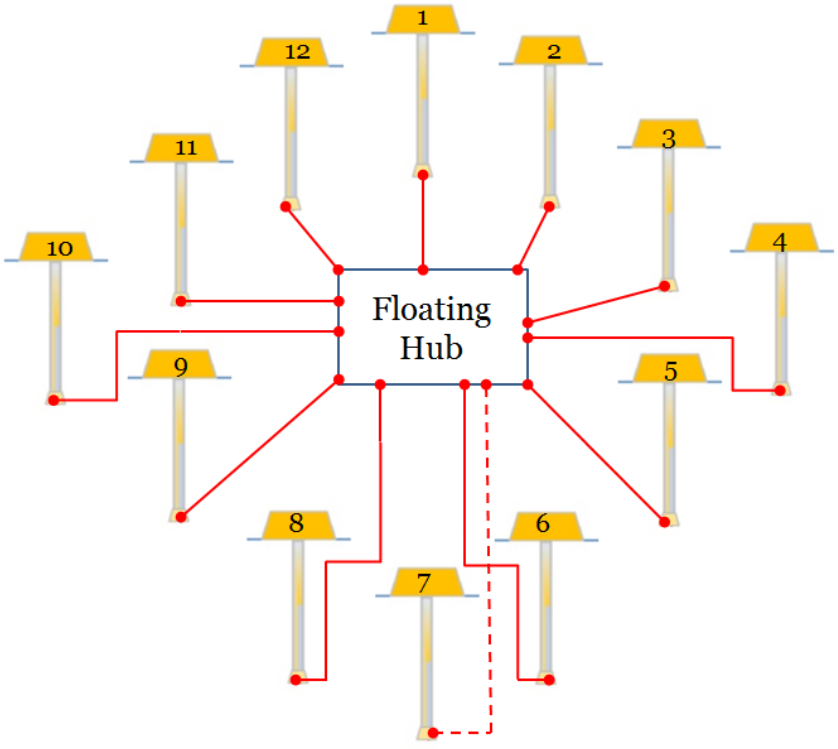

Figure 35: 12-Radial scheme

5.3. Transmission Cable

In order to connect various WECs together, radial scheme is adopted and shown in the figures in previous clause. The interconnection between these WECs will be done with the help of cables. These cables are selected so that they can withstand the extreme environment of the sea and deliver the power effectively. The figure below shows the selected cable type'

Figure 36: Armored Cable

The cable is a cross-linked polyethene (XLPE) insulated. The sheath is made up of poly vinyl chloride (PVC) and the steel wire armor provides the mechanical strength to the cable. This cable is capable to withstand the extreme submarine environment and can function well if laid on the sea bed. The basic details of the cable is given below

Table 1: Cable details

Voltage Level (kV)	0,6-1
Conductor	Copper
Insulation	Cross-linked polyethene (XLPE)
No. of cores	3
Armor	Galvanized steel
Sheath	Poly vinyl chloride (PVC)
Standard conformance	IEC-60502

This cable type will suit well for the low voltage application as the voltage level is 0,4 kV.
Cable dimensions and the technical details are given in the Appendix A.

5.4. Cable model

In order to find the best radial scheme to be adopted for the WECs, it is important to analyze the system. For the purpose cable parameters will be calculated to observe the losses in the cable. The cable model is given in fig 31, which is further simplified in fig 32.

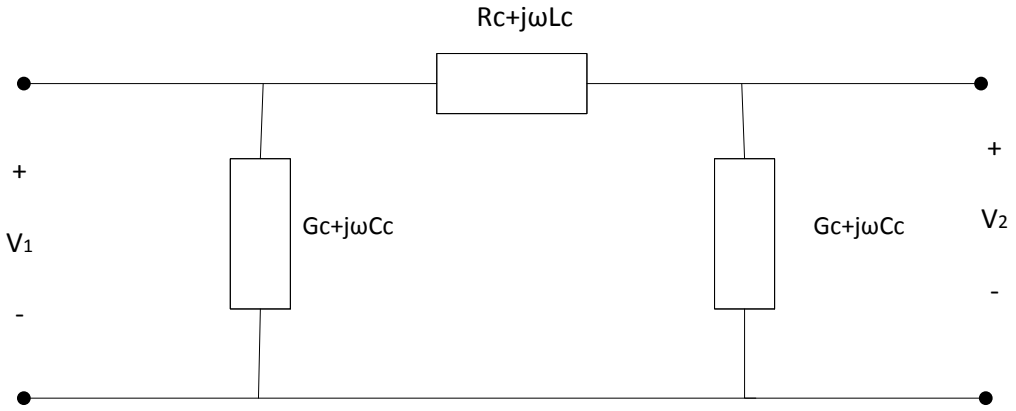

Figure 37: Cable model

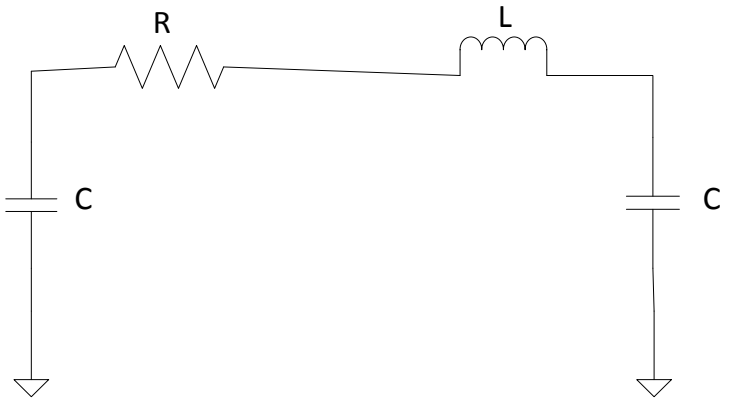

Figure 38: Simplified Cable model

The cable parameters are defined below

$R = Resistance\ due\ to\ resistivity\ of\ copper\ conductor$

$L = Inductance\ due\ to\ magnetic\ field\ surrounded\ by\ the\ copper\ conductors$

$C = Capacitance\ due\ to\ electrical\ field\ between\ copper\ conductors\ and\ conductors\ and\ ground$

These parameters can be represented mathematically by the following equations

Cable capacitance

$$C = \frac{\varepsilon_r}{18.\, ln\left(\frac{r_I}{r_c}\right)} \quad {\mu F}/{km}$$

Cable inductance (self)

$$L_s = \frac{\mu_0 \mu_r}{2\pi}\, ln\left(\frac{r_I}{r_c}\right) + \frac{\mu_0 \mu_r}{8\pi} \quad {H}/{m}$$

Cable inductance (Mutual)

$$L_M = 0.05 + 0.2\, ln\left(\frac{K.s}{r_c}\right) \quad {mH}/{km}$$

Metal resistivity

$$\rho_{cu} = 1{,}72 * 10^{-8}\, \Omega - m$$

Actual resistivity

$$\rho = \frac{(r_c * r_c * \pi * \rho_{cu})}{A_{cable}}$$

$$\rho = 1{,}765 * 10^{-8}\, \Omega - m$$

Cable resistance

$$R = \frac{\rho * l}{r_c * r_c * \pi}\, \Omega$$

In order to calculate the above parameters the cable dimensions are formulated and are represented in Appendix B.

5.5. Conclusion

Radial scheme for the interconnection of several WECs is briefly discussed and will be made basis for the system analysis. The selection of the radial scheme is based on the fact that it reduces the cable length and effectively transmits the power to the floating hub. The cables used for the interconnection links must be capable to withstand the extreme environment of the sea. Galvanized steel wire armored cables with XLPE provides the strength and performance to keep the system secure and efficient. Cable parameters are significant entities in order to find the losses in the transmission media.

6. System Analysis

In order to investigate the most efficient and reliable radial scheme, system´s performance must be analyzed. The radial schemes discussed in the previous chapter will be considered. It is important to observe the system for the following constraints

- Power losses in the transmission media.
- Voltage drop per radial of the scheme.
- Cost analysis of each radial scheme under observation

6.1 Power loss

It is important to calculate the power loss in the transmission media as the transmission structure is a vital part of the system. The cables used for the purpose exhibit certain power loss. With reference to the Clause 5.4, the cable model adopted for the loss evaluation is presented. The cable parameters such as, capacitive reactance, inductive reactance and the resistance of the copper conductors is calculated in Appendix B.

It is clear from the calculation that the inductive reactance is very low as compared to the resistance of the copper conductors. This can then be neglected. Furthermore the capacitive reactance is very large as compared to the resistance of the copper conductors. It can then be concluded that the power loss can be simplified to the form shown in the equation below

$$P_{loss} = I^2 R \tag{6.1}$$

The power loss can be simplified to the current squared times the resistance of the copper conductor. Two conditions will be observed and are given below

- Power loss at maximum power output from each WEC connected in radial topology
- Power loss at normal loading at each WEC connected in radial topology

Maximum power output is the maximum rated output of the generators in WECs. The normal power output refers to a situation when the WECs are loaded normally.

6.1.1 Power loss at maximum power output

The maximum power generation from a single WEC is 30 kW. If the maximum power output is considered with power factor (PF) of 0.8 the power losses exhibited by each radial scheme is presented in the table below

Table 2: Maximum power loss

Radial Scheme	Max power Loss (W)	% of total power (360 kW 3-phase)
2	14313,817	11,91
4	12255,55	10,2
6	11851,875	9,87
12	12 093,750	10,07

As mentioned in the system definition, 12 WECs are considered to be connected in each radial scheme. For the case of 30 kW output from an individual buoy, the maximum power output from one radial scheme with 12 WECs will be 360 kW. It is evident from the table 1 that the power loss decreases with increasing the number of radials. It can be seen in the figure below

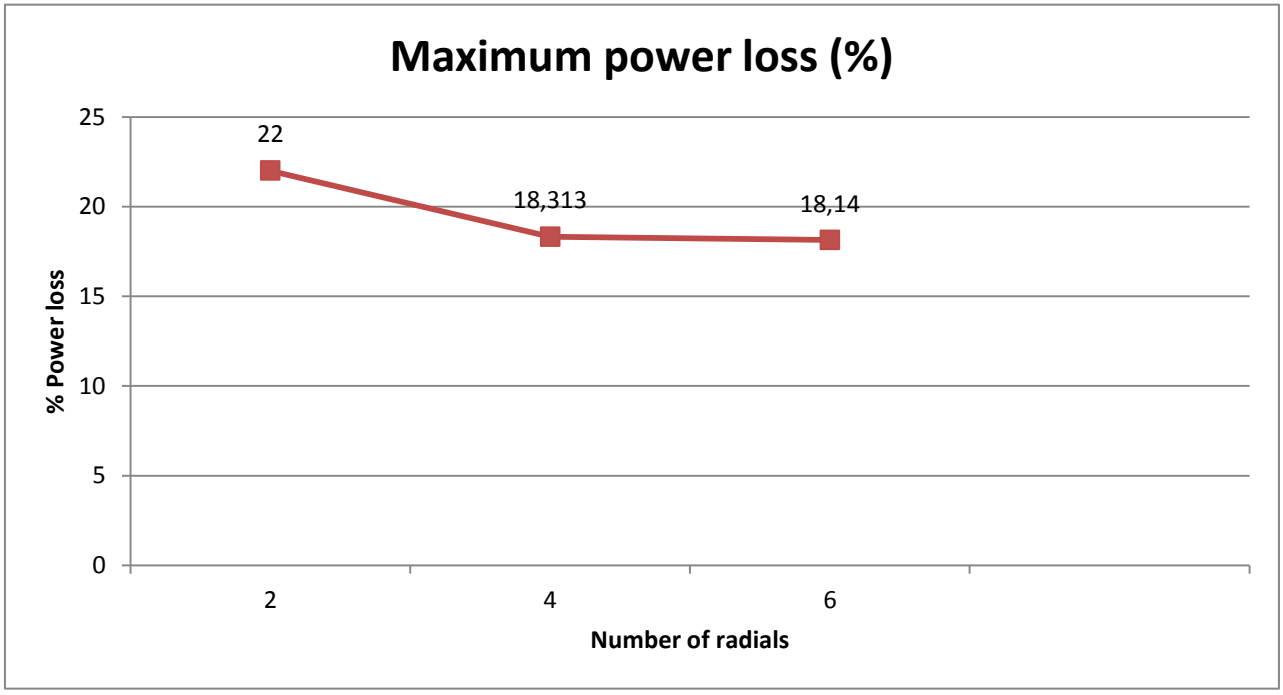

Figure 39: Maximum power loss chart

The maximum power loss in the fig 33 decreases with increased number of radials. However, the total allowable power loss is in the range of 5% in the case if maximum power output is considered.

6.1.2 Power loss at normal loading

In practical scenario the WEC will not always generate maximum power. This is due to the fact that the wave condition in the sea is unpredictable and to attain maximum power is very intermittent. Assuming a loading of 10 kW on each WEC, the overall output of 12 WEC interconnected system would yield 120 kW. This case is more practically viable and will give an idea about the power loss in the actual sea condition. The power loss in the normal loading condition is presented in the following table

Table 3: Power loss at normal loading condition

Radial Scheme	Power loss at normal loading (W)	% of total power (120 kW 3-phase)
2	1590,424	3,96
4	1361,667	3,39
6	1316,875	3,27
12	1343,750	3,35

It is observed in the table 2 that the power loss is decreasing as the number of radials is increased. This follows similar trend as observed previously in the maximum power loss case. The exception is that the power loss calculated in the normal loading case is well in the defined limit (i-e. 3% power loss at normal loading). It is important to mention here that the power loss slightly increases as we go from 6 radial to 12 connections per system. This is due to the fact that the cable resistance calculated in the case of 6- radial system is lesser then that of 12 connection system resulting a slight increase in the power loss. Power loss calculation details are given in Appendix C.

This can be graphically observed in figure 34

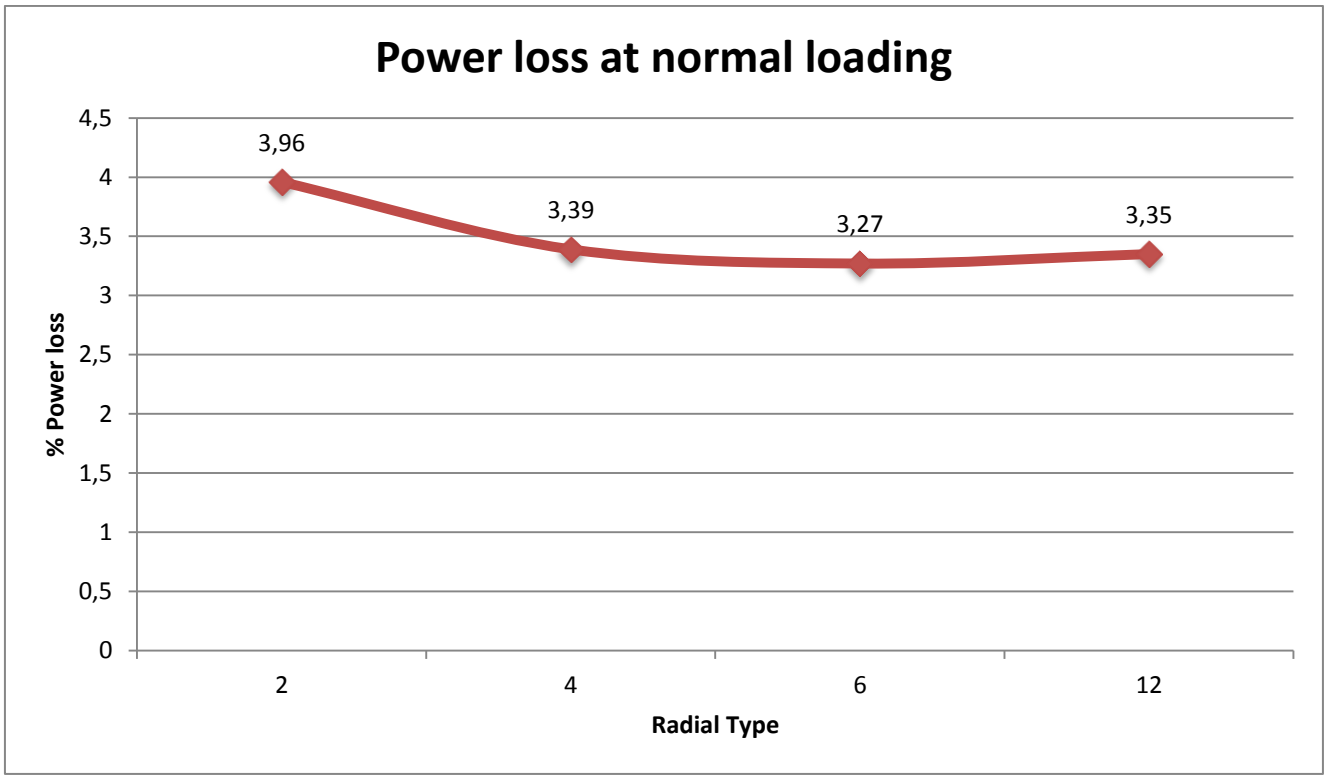

Figure 40: Power loss at normal loading

6.2 Voltage drop

System analysis includes voltage drop calculation which is important to inspect the performance of the system. Similar to the approach adopted in the case of power loss calculation, the voltage drop at one terminal of a radial can be presented by the following equation

$$U_1 = U_2 + I(R + j\omega L) \tag{6.2}$$

It is evident from the above equation that the voltage drop depends upon the resistance of the copper conductors and the inductive reactance of the cable. Phase angle will be involved in the calculation which can be computed by the power factor. PF 0.8 is assumed for the calculation. The trail calculation shows that the difference in the phase angle at the two terminals is very small and can be neglected. This shows that the voltage drop per radial can be simplified as

$$U_{drop} = I * R \tag{6.3}$$

The trail calculation is made in the Appendix D. The radial schemes under consideration will be examined to calculate the voltage drop per radial per phase of the system.

6.2.1 Voltage drop for 2-radial scheme

In the case of 2-radial system the voltage drop calculation is presented in the table below

Table 4: Voltage drop/radial/phase for 2-Radial scheme

Radial scheme type.	Connection	Current (A)	Resistance (ohm)	Max Voltage drop (V)	Normal Loading (kW)	Current at PF (0,8)	Voltage drop at Normal Loading (V)
2	1_2	54,13	0,34	18,62	10,00	18,04	6,21
2	2_3	108,25	0,08	8,94	20,00	36,08	2,98
2	3_4	162,38	0,04	6,70	30,00	54,13	2,23
2	4_5	216,51	0,03	6,38	40,00	72,17	2,13
2	5_6	270,63	0,02	4,65	50,00	90,21	1,55
2	6_0	324,76	0,01	4,47	60,00	108,25	1,49

The voltage drop calculated in the above table is for the single radial in the 2-radial system. The total voltage drop will be twice the voltage drop for the single radial i-e.

$$Voltage\ Drop = 16{,}59\ V$$

The % voltage drop/radial/phase of the system is

$$\%\ Voltage\ drop = \frac{16{,}59}{231} = 7{,}18\%$$

6.2.2 Voltage drop for 4-radial scheme

The voltage drop calculation for 4-radial system can be observed in table 3. The voltage drop calculation is carried out for per radial per phase of the system. The total voltage drop over one radial will be the sum of the voltage drop over each link in the radial.

Table 5: Voltage drop/radial/phase for 4-Radial scheme

Radial Scheme type.	Link. No	Connection	Current (A)	Resistance (ohm)	Max Voltage drop (V)	Normal Loading (kW)	Current at PF (0,8)	Voltage drop at Normal Loading (V)
4	1	1_2	54,13	0,34	18,62	10,00	18,04	6,21
4	5	2_3	108,25	0,08	8,94	20,00	36,08	2,98
4	9	3_0	162,38	0,04	6,70	30,00	54,13	2,23

The total voltage drop over one radial will be

$$Voltage\ drop\ =\ 11{,}42\ V$$

The total voltage drop for the other radials would be the same. The percentage voltage drop per radial per phase will be

$$\%\ Voltage\ drop = \frac{11{,}42}{231} = 4{,}94\%$$

6.2.3 Voltage drop for 6-radial scheme

The voltage drop for 6-radial scheme is calculated and presented in the table below

Table 6: Voltage drop/radial/phase for 6-Radial scheme

Radial scheme type.	Link. No	Connection	Current (A)	Resistance (ohm)	Max Voltage drop (V)	Normal Loading (kW)	Current at PF (0,8) (A)	Voltage drop at Normal Loading (V)
6	1	1_2	54,13	0,34	18,62	10,00	18,04	6,21
6	5	2_3	108,25	0,08	8,94	20,00	36,08	2,98

The voltage drop per radial per phase for the 6-radial scheme will be the sum of the voltage drop over each link i-e.

$$Voltage\ drop = \ 9{,}19\ V$$

Voltage drop over the other radials will be the same. The percentage voltage drop per radial per phase is

$$\%\ Voltage\ drop = \frac{9{,}19}{231} = 3{,}97\%$$

6.2.4 Voltage drop over 12 connections to floating hub

The voltage drop for 12 connections to the floating transformer hub is given in the table below

Table 7: Voltage drop/radial/phase for 12-connection scheme

Radial scheme type.	Link. No	Connection	Current (A)	Resistance (ohm)	Voltage drop (V)	Normal Loading (kW)	Current at PF (0,8)	Voltage drop at Normal Loading (V)
12	1	1_2	54,13	0,34	18,62	10,00	18,04	6,21

The voltage drop per connection per phase for the 12 individual connection scheme will be the sum of the voltage drop over single link connecting the WEC to the floating transformer hub i-e.

$$Voltage\ drop = 6{,}21\ V$$

The voltage drop over the other 11 connections will be the same. The percentage voltage drop per connection per phase is

$$\%\ Voltage\ drop = \frac{6{,}21}{231} = 2{,}68\%$$

It is evident from the above calculation that voltage drop decreases as the number of radials are increased. This can be observed graphically in the chart below

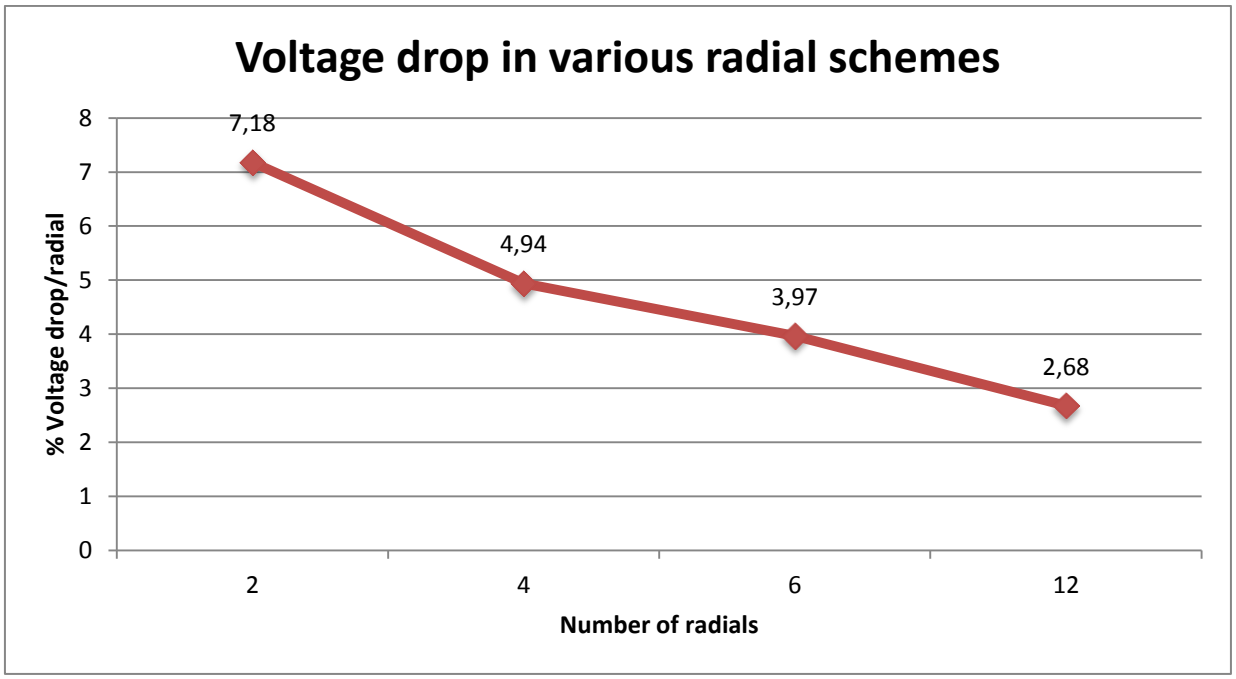

Figure 41: Voltage drop for various radial schemes

6.3 Cost Analysis

Economics is key aspect in system evaluation. It is vital to select a system which is economically sustainable. The standard components and the transmission media will ensure economically feasible system solution. Speaking of the economics the most prominent component in the system is the transmission cables. The cables used for the loss evaluation is manufactured by *Universal Cables.* The cable data regarding the design and cost and the calculation is given in [20]. The approximated transmission cable cost for 2, 4, 6-radials and 12-connections to the floating hub is given in the table below

Table 8: Actual and estimated Cable cost

Radial scheme	**Actual cable cost (SEK)**	**Estimated Cable cost (Incl. fittings, joints etc.) (SEK)**
2	83818,08	167636,16
4	42202,08	84404,16
6	31903,20	63806,40
12	23811,84	47623,68

The actual cost is based on the existent manufacturer´s price. The transmission system also included cable joints, fittings, housings, floats, weights etc. these are not included in the actual cost. The approximation of the total cabling system is given as estimated cable cost.

6.4 Conclusion

The system analysis consisting of power loss evaluation, voltage drop calculation and the cost analysis depict that the system with more radials is better under the context of performance, effectiveness and economics. The power loss and the voltage drop in the normal loading case decrease as the number of radials are increased. This can be observed in the chart below.

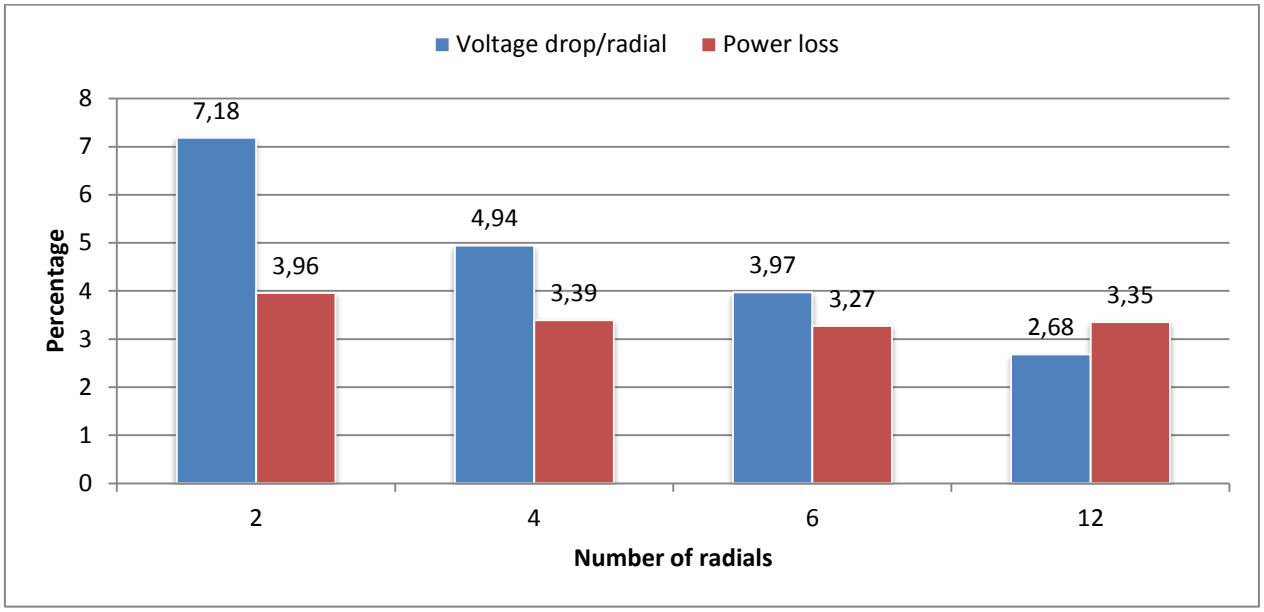

Figure 42: Power loss and voltage drop for various radial schemes

Similarly the chart below represents the transmission cable cost for the system

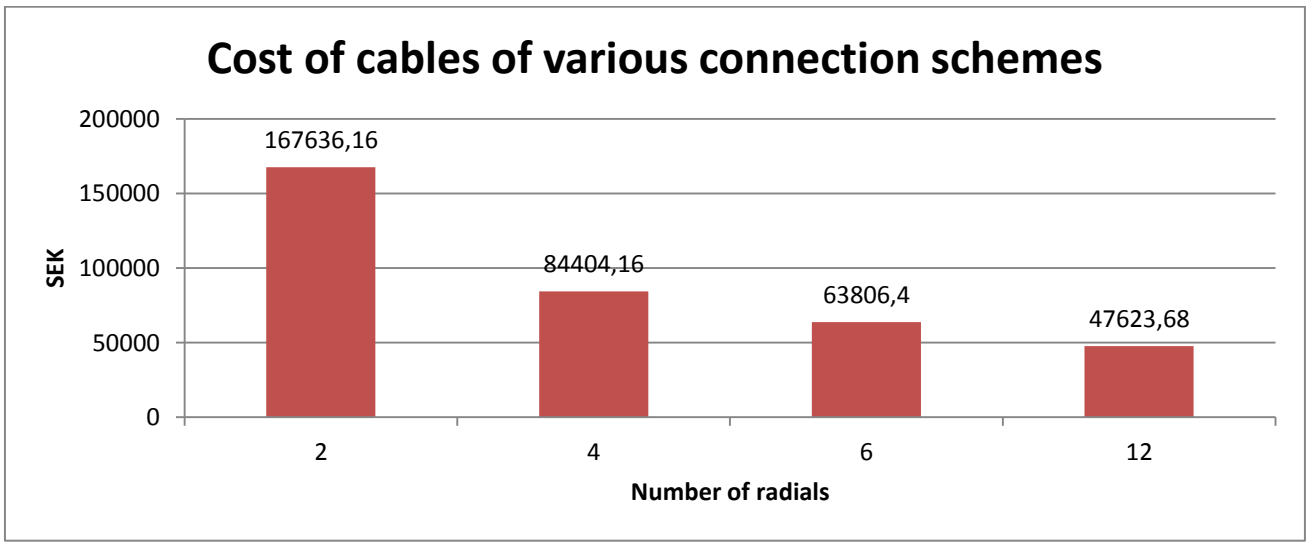

Figure 43: Transmission cable cost for various radial schemes

It can be concluded that system with 6-radials or 12 individual connections to the floating transformer hub can prove to be effective and economical selection.

7. Windfarm and Wavefarm Comparison

In the previous section it is evident that the 6-radial scheme or 12 connections to the floating hub can be feasible and economical solution to interconnect 12 WECs. The power loss and the voltage drop presented in the previous section shows that more number of radials will effectively reduce the losses and increase the performance of the system. In the case of 12 connections to the floating hub, it is observed that the power losses slightly increase due to the fact that the cable rating is higher as compared to the 6-radial system.

In order to compare a Windfarm with a wavefarm, it is necessary to define the basis of the comparison. The basis of the comparison will be power density calculation and power generation cost.

Table 9: Technical specifications of windfarm and wavefarm

Energy Source	Wind	Wave
Total power	130 MW	130 MW
Power of each unit	3 MW	300 kW
No. of units	43	430
Voltage level (kV)	30	0,4
Distance between units	700m	40m
Rotor Diameter	90m	-

Table 8 describes the technical specifications of windfarm and the wavefarm. The comparison is done for 130 MW maximum power. In the case of windfarm one unit will be of 3 MW, therefore 43 units will collectively produce 13o MW. Similarly a single unit in the case of wavefarm will be rated as 300 kW, therefore 430 units will collectively produce a total power of 130MW. One important element here is the distance between the units. In the case of windfarm, the distance between two 3MW wind turbines is about 7-10 times the rotor diameter. The wind turbine under consideration is manufactured by VESTAS and the technical data is presented in the Appendix.

In order to carry out the comparison it is important to look for a solution for a higher power level for wavefarm. In the previous discussion the maximum power output from a single WEC was 30 kW. Now for the comparison this power level needs to be increased 10 times. It is important to inspect if standard solutions exist for 300 kW WEC.

7.1 300 kW Wave Energy Converter

The power level now is 10 times higher as compared to the previous analysis. This increase in the power level will not change the calculation pattern. The assumptions for a 300 kW WEC will be

- 300 kW Maximum power output
- 40 m distance between individual buoys
- 10 units in total
- 0,4 kV voltage level

The difference between the 30 kW and the 300 kW case is the distance between the individual WECs. In this case two 300 kW WECs will be separated by a distance of 40m. The voltage level is the same i-e. 0,4 kV. Another difference is the total number of units to be interconnected. In this case 10 WECs are selected to produce total power of 3 MW. Hence one 3 MW wavefarm will consist of 10 WECs each with the maximum power of 300 kW.

As discussed in the previous section that the radial scheme with 6-radials is feasible and viable solution for the interconnection. The system with 10 WECs connected in radial scheme will consist of 5-radials. This can be observed in fig 38.

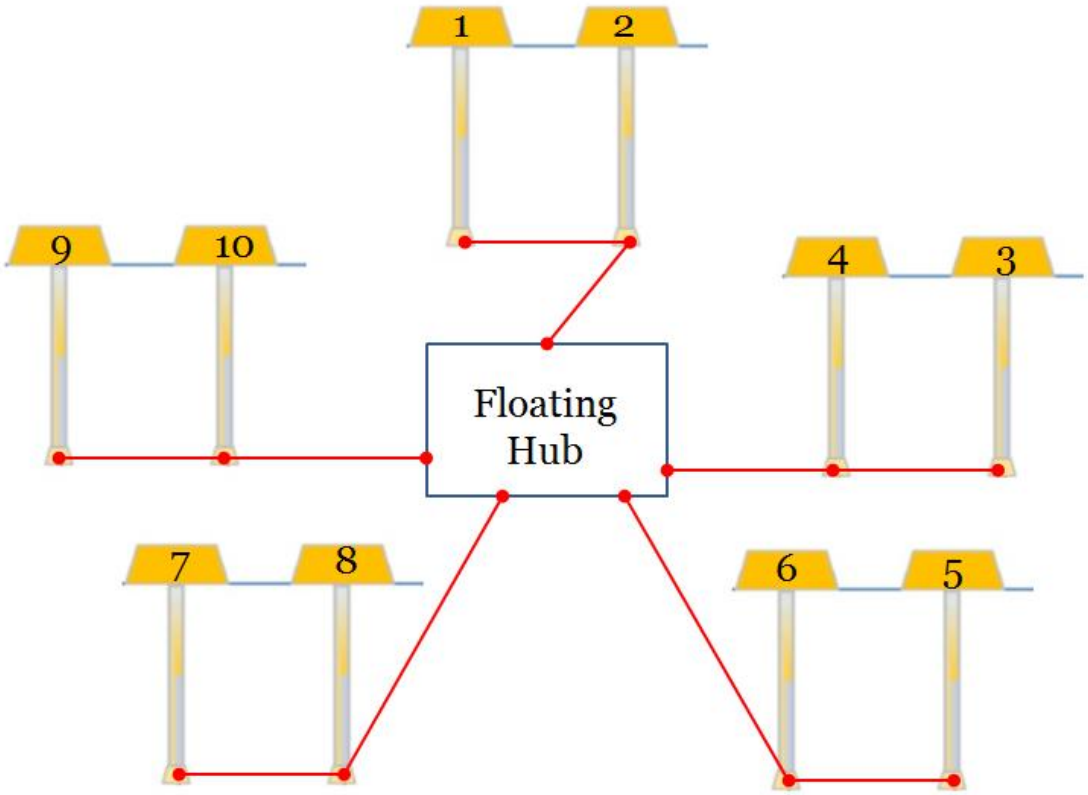

Figure 44: 5-radial scheme for 3MW wavefarm

It can be seen in the above figure that a total of 10 WECs are connected in 5 radials, collectively producing a total power of 3MW. The power losses and the voltage drop for 3MW wavefarm is calculated in the table below

Table 10: Power loss and voltage drop for 3MW wavefarm

Radial Scheme	Max power Loss (W)	% of total power loss (3 MW 3-phase)	Power loss at normal loading (W)	% of total power (700 kW 3-phase)	Voltage drop (V)/phase/Radial
5	22171,875	3,17	7,48	4,05	8,20 (3,55%)

The calculation of power loss and voltage drop is based on the similar simplified model as discussed in the previous section. It can be observed that the power loss and voltage drop lie within the permissible limits.

The cables for the transmission purpose are manufactured by the same company as described in clause 5.3. In this case the rating of the cable is higher due to increased power level. It is worth noting here that the solution for the electrical generator for 300 kW wave energy converter is also available. Synchronous reluctance machine with maximum output of 315 kW manufactured by ABB can be an efficient and feasible selection. Technical details of the synchronous reluctance generator are presented in the Appendix.

7.2 3MW Windfarm and Wavefarm comparison

In order to compare the power densities of windfarm and wavefarm, it is important to observe the spacing between the two turbines. The energy loss associated with the geometry of the windfarm is termed as array loss [21]. These losses can be effectively decreased if the geometry of the wind turbines is optimized. This geometry of wind turbine placement is the vital element that affects the total energy loss. It has been observed that distance between two wind turbines is of the order of 8-10 rotor diameters [21]. The wind turbine under consideration is manufactured by VESTAS and has a rotor diameter of 90 m [22]. This can be visualized from the figure below

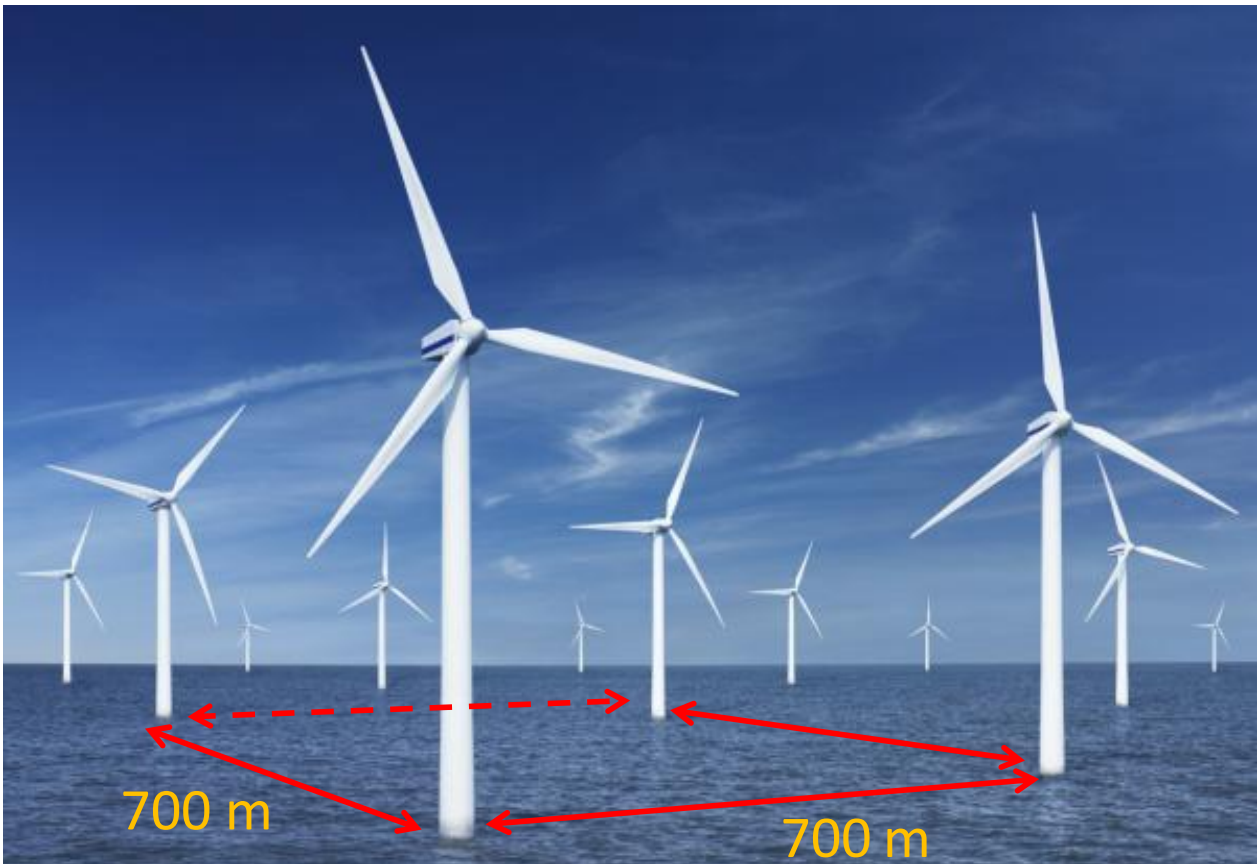

Figure 45: Wind turbine spacing

Clearing distance of 700m is approximated between two 3MW wind turbines. The total area surrounded by two 3MW wind turbines will be 490000m^2. On the contrary a 3MW wavefarm would surround an area of approximately 122500m^2. This can be seen in the figure below

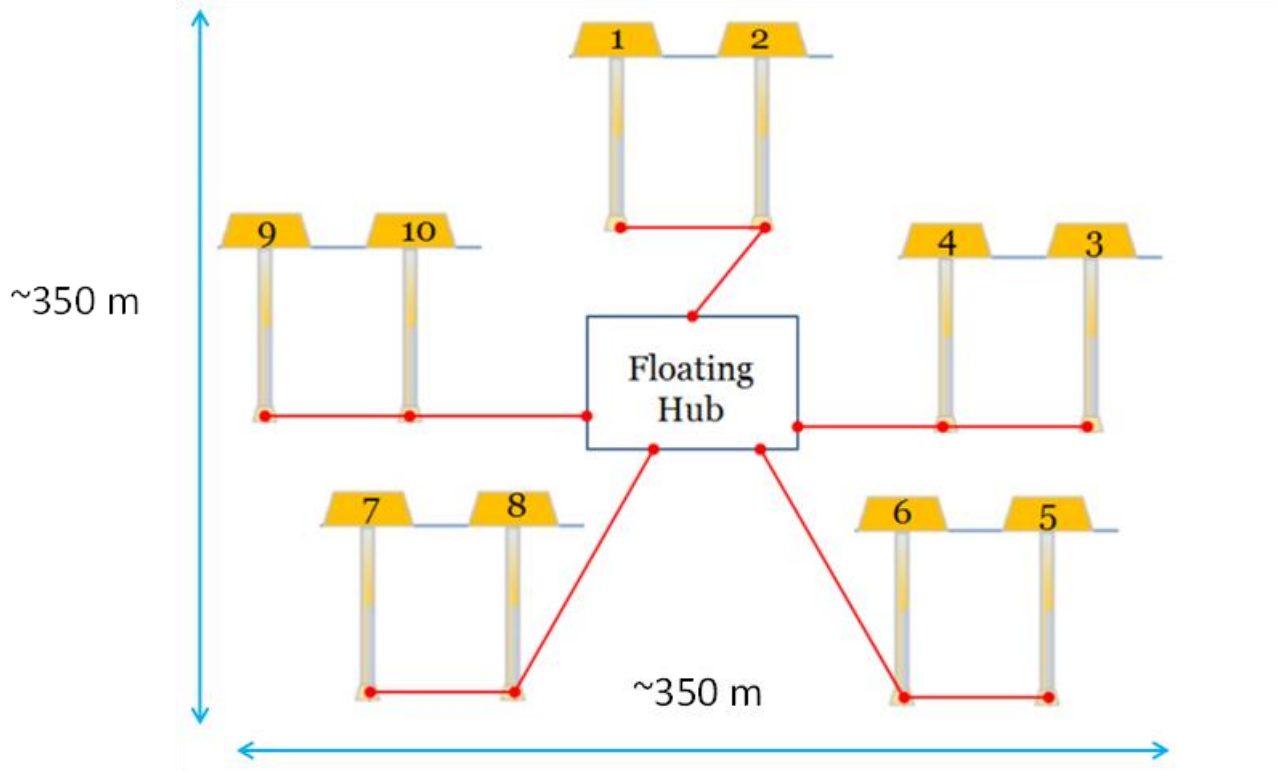

Figure 46: 3MW Wavefarm geometry

7.3 Conclusion

It is evident from the above comparison that the wavefarm of similar power rating as windfarm has an enhanced power density. In the case above the 3MW wavefarm constituting of 10, 300 kW WECs can produce similar power output, covering ¼ of the area between two 3MW wind turbines. This shows that the wavefarm has 4 times higher power generation capability.

It is important to note that the maximum power output in the case of a windfarm and wavefarm is very intermittent. The calculation presented above is based on the maximum power capability. The wind condition at a particular site is very different from another location. Similarly in the case of wave energy, the wave occurrence is very different and depends upon the location of installation. The actual comparison can therefore be established on actual site conditions.

8. Conclusions and Future Work

The theme of this project is to carry out a research on the design and performance of electrical system of a wavefarm. This includes the design of the electrical system and its components such as generator and frequency converter. The device used as the basis of research is heaving device called WaveEL Buoy manufactured by Waves4power, a Swedish company. The focus of this company is to develop solutions for wave power technology and wavefarms. In order to design and analyze the system it is important to select standard system components. In order to fulfill this purpose ABB Västeräs is assisted this project as a reference group and provided the technical expertise required for the standard solution for the wavefarm design. The project is based on two parts, first to design an electrical system with low power level and analyze it. Second part included a higher power level design of the wavefarm. Finally a comparison is carried out between windfarm and wavefarm.

It can be concluded from the results and findings of the project that,

- Synchronous reluctance machine is efficient, compact and viable option for the generator to be mounted inside the WaveEL Buoy. It shows better torque capability, lesser losses and is less massive then the conventional induction machine of similar ratings.
- IGBT based frequency converter manufactured by ABB provide enhanced stability and control over the generator. It is compatible with various other electrical generators and hence provides the compatibility with the system.
- Transmission of power to the floating hub is done using 50Hz AC link from the WaveEL Buoy. This facilitates the auxiliary power flow over the same transmission infrastructure.
- Synchronous reluctance generator and ABB´s ACSM1-204 with ACS850-04 frequency converter module for 30 kW wave energy converter is an appropriate and effective choice of the electrical conversion system.
- Transmission cable proposed for the system is mechanically strong enough to cope with the extreme marine environment.
- Interconnection of the wave energy converters is a vital part that governs the effective and efficient power transfer from the WECs to the floating hub. Radial scheme is used to lower the cable length without compromising the power transfer in the system.
- System with 6-radials or 12-individual connection to the floating transformer hub is a viable choice as it displays lesser power loss in the transmission media and voltage drop over each radial in the system.
- Transmission cable cost is reduced when more number of radials is included in the system.

- Standard solution with ABB´s synchronous reluctance generator and frequency converter is available for higher power level. Hence 300 kW power level can be achieved.
- Wavefarm exhibits 4 times better power density then equally rated windfarm at maximum power output. Practical results will be based on actual site conditions
- Installation cost for a 3MW wavefarm is lesser then 3MW windfarm.

Above mentioned conclusions make it evident that research in the field of wave power will open new horizons in the field of electrical power and generation of electricity from renewable energy resources.

Future Work

Future development in conjunction to this project work are listed below

- Power produced can be used locally, i-e. Storage by charging of batteries.
- Small population nearby the shore can be fed with the power produced by the wavefarm except feeding it to the grid.
- A system can be developed to charge the batteries of the boats. A charging platform design can be developed and fed with the power generated from wavefarm.
- Power can be supplied to offshore rigs for pumping and drilling processes.
- Protection scheme can be designed to protect the system from the faults and short circuits.
- Sea based cables can be manufactured on low voltage level that could withstand the intense environment of the ocean/sea.
- Wave forecasting algorithm can be generated in order to obtain better output from the WECs.

APPENDIX A

Cable dimensioning

We suppose a current rating of 70-75A. Here I am initially starting with the single connection of the 6-radial system that I discussed earlier. According to the Universal cable data the cross section of the cable is 6 mm^2. The calculation is based on the international standard IES 60502-1 [23].

$$A_L = 6\,mm2$$

$$d_L = 2.8\,mm$$

Considering XLPE Insulation

$$Thickness\ of\ the\ insulation = tI = 0.7\,mm$$

We consider a metallic sheath around insulation

$$A_{sheath-m} = A_{SM} = 1.5\,mm2$$

Then the increase in diameter would be 0.5 mm

$$t_{sheath} = 0.5\,mm$$

$$Core\ diameter = Dc = d_L + 2tI + t_{sheath}$$

$$Dc = 4.7\,mm$$

Diameter over laid up conductor

$$D_f = kDc$$

As number of cores = 3

$$k = 2.16$$

$$D_f = 10.15\,mm$$

Considering extruded inner covering and/or filler

$$t_{ex-cover-in} = t_{ex} = 1mm$$

$$D_{ex} = D_f + 2t_{ex}$$

$$D_{ex} = 12.15\ mm$$

$$D_u = 12.15\ mm$$

The separation sheath is

$$D_s = 1.04\ D_u + 1.2$$

$$D_s = 13.836\ mm$$

The armor wire diameter is

$$d_{AW} = 1.25\ mm$$

$$D_x = D_s + 2t_a$$

$$D_x = 16.36\ mm$$

Thickness of outer sheath

$$t_{os} = 0.035\ D + 1$$

$$t_{os} = 1.57\ mm$$

The overall diameter hence

$$D_o = D_X + 2t_{os}$$

$$D_o = 19.533\ mm$$

The overall diameter is approximately equal to the actual diameter given in [24].

Diameter calculation for the other current ratings is done in MS Excel and given below

Current rating

Current rating is calculated from apparent power using PF 0.8.

Radial Scheme Type.	Link. No	Connection	Length (M)	Power (Kw)	App. Power PF=0,8	Voltage (kV)	Current (A)	Conductor Type
2	1	1_2	120,000	30,000	37,500	0,400	54,127	Copper
2	2	7_8	120,000	30,000	37,500	0,400	54,127	Copper
2	3	2_3	120,000	60,000	75,000	0,400	108,253	Copper
2	4	8_9	120,000	60,000	75,000	0,400	108,253	Copper
2	5	3_4	120,000	90,000	112,500	0,400	162,380	Copper
2	6	9_10	120,000	90,000	112,500	0,400	162,380	Copper
2	7	4_5	120,000	120,000	150,000	0,400	216,506	Copper
2	8	10_11	120,000	120,000	150,000	0,400	216,506	Copper
2	9	5_6	120,000	150,000	187,500	0,400	270,633	Copper
2	10	11_12	120,000	150,000	187,500	0,400	270,633	Copper
2	11	6_0	120,000	180,000	225,000	0,400	324,760	Copper
2	12	12_0	120,000	180,000	225,000	0,400	324,760	Copper

Cable cross-section

The cable cross section is selected form IEC 60502-1 [23].

Radial scheme type.	Link. No	Connection	Cable cross-section	nominal diameter of the core (mm)	Thickness of the insulation (mm)	Thickness of the sheath (mm)	Diameter of the core (mm)
2	1	1_2	4,000	2,300	0,700	0,500	4,200
2	2	7_8	4,000	2,300	0,700	0,500	4,200
2	3	2_3	16,000	4,500	0,700	0,500	6,400
2	4	8_9	16,000	4,500	0,700	0,500	6,400
2	5	3_4	35,000	6,700	0,900	0,500	9,000
2	6	9_10	35,000	6,700	0,900	0,500	9,000
2	7	4_5	50,000	8,000	1,000	0,500	10,500
2	8	10_11	50,000	8,000	1,000	0,500	10,500
2	9	5_6	70,000	9,400	1,100	0,500	12,100

2	10	11_12	70,000	9,400	1,100	0,500	12,100
2	11	6_0	95,000	11,000	1,100	0,500	13,700
2	12	12_0	95,000	11,000	1,100	0,500	13,700

The overall diameter of the cable connection for a 2-radial system is given below

Diameter over laid up conductors (mm)	**Thickness of extruded inner covering (mm)**	**Diameter with extruded covering (mm)**	**Diameter with separation sheath (mm)**	**Diameter of the armour wire (mm)**	**Diameter with armour (mm)**	**Thickness of outer sheath (mm)**	**Overall diameter of the cable (mm)**
9,072	1,000	11,072	12,715	1,250	15,215	1,533	18,280
9,072	1,000	11,072	12,715	1,250	15,215	1,533	18,280
13,824	1,000	15,824	17,657	1,600	20,857	1,730	24,317
13,824	1,000	15,824	17,657	1,600	20,857	1,730	24,317
19,440	1,600	22,640	24,746	1,600	27,946	1,978	31,902
19,440	1,600	22,640	24,746	1,600	27,946	1,978	31,902
22,680	1,800	26,280	28,531	2,000	32,531	2,139	36,808
22,680	1,800	26,280	28,531	2,000	32,531	2,139	36,808
26,136	2,000	30,136	32,541	2,000	36,541	2,279	41,099
26,136	2,000	30,136	32,541	2,000	36,541	2,279	41,099
29,592	2,000	33,592	36,136	2,500	41,136	2,440	46,015
29,592	2,000	33,592	36,136	2,500	41,136	2,440	46,015

APPENDIX B

Electrical parameters such as resistance, capacitance and the inductance are calculated in the table below. The required dimensions of the cable are also computed.

Radial Scheme type.	Link No	Connec-tion	Radius of the conductor r_i (mm)	Radius of the conductor r_c (mm)
2	1	1_2	1,850	1,150
2	2	7_8	1,850	1,150
2	3	2_3	2,950	2,250
2	4	8_9	2,950	2,250
2	5	3_4	4,250	3,350
2	6	9_10	4,250	3,350
2	7	4_5	5,000	4,000
2	8	10_11	5,000	4,000
2	9	5_6	5,800	4,700
2	10	11_12	5,800	4,700
2	11	6_0	6,600	5,500
2	12	12_0	6,600	5,500

The cable parameters can be observed below

Radial scheme type.	Link. No	Con-nec-tion	Cable Capaci-tance (µF/km)	Actual Capac-itance (µF)	Mutual Induct-ance (mH/km)	Actual In-ductance (mH)	Self Induct-ance (H/m)
2	1	1_2	0,292	0,035	0,503	0,060	1,451E-07
2	2	7_8	0,292	0,035	0,503	0,060	1,451E-07
2	3	2_3	0,513	0,062	0,440	0,053	1,042E-07
2	4	8_9	0,513	0,062	0,440	0,053	1,042E-07
2	5	3_4	0,584	0,070	0,432	0,052	9,759E-08
2	6	9_10	0,584	0,070	0,432	0,052	9,759E-08
2	7	4_5	0,622	0,075	0,427	0,051	9,463E-08
2	8	10_11	0,622	0,075	0,427	0,051	9,463E-08
2	9	5_6	0,660	0,079	0,422	0,051	9,206E-08
2	10	11_12	0,660	0,079	0,422	0,051	9,206E-08
2	11	6_0	0,762	0,091	0,412	0,049	8,646E-08
2	12	12_0	0,762	0,091	0,412	0,049	8,646E-08

Radial scheme type.	Link. No	Connection	Capacitive reactance (ohm)	Inductive reactance (ohm)	Metal resistivity (ohm-m)	Actual Resistivity)ohm-m)	Resistance (ohm)
2	1	1_2	8,962E+09	0,019	1,72E-08	1,787E-08	0,516
2	2	7_8	8,962E+09	0,019	1,72E-08	1,787E-08	0,516
2	3	2_3	5,106E+09	0,017	1,72E-08	1,710E-08	0,129
2	4	8_9	5,106E+09	0,017	1,72E-08	1,710E-08	0,129
2	5	3_4	4,485E+09	0,016	1,72E-08	1,733E-08	0,059
2	6	9_10	4,485E+09	0,016	1,72E-08	1,733E-08	0,059
2	7	4_5	4,206E+09	0,016	1,72E-08	1,729E-08	0,041
2	8	10_11	4,206E+09	0,016	1,72E-08	1,729E-08	0,041
2	9	5_6	3,964E+09	0,016	1,72E-08	1,705E-08	0,029
2	10	11_12	3,964E+09	0,016	1,72E-08	1,705E-08	0,029
2	11	6_0	3,437E+09	0,016	1,72E-08	1,721E-08	0,022
2	12	12_0	3,437E+09	0,016	1,72E-08	1,721E-08	0,022

APPENDIX C

Power loss at maximum and normal loading for 2- radial system is calculated in the table below. Similar calculations can be observed for the other radial schemes

Radial scheme type.	Link. No	Connection	Current (0.8) (A)	Resistance (ohm)	Max Power Loss (W)	Normal Loading (kW)	Current at normal loading (A)	Power Loss at normal loading (W)
2	1	1_2	54,127	0,516	1 511,719	10,000	18,042	167,969
2	2	7_8	54,127	0,516	1 511,719	10,000	18,042	167,969
2	3	2_3	108,253	0,129	1 511,719	20,000	36,084	167,969
2	4	8_9	108,253	0,129	1 511,719	20,000	36,084	167,969
2	5	3_4	162,380	0,059	1 554,911	30,000	54,127	172,768
2	6	9_10	162,380	0,059	1 554,911	30,000	54,127	172,768
2	7	4_5	216,506	0,041	1 935,000	40,000	72,169	215,000
2	8	10_11	216,506	0,041	1 935,000	40,000	72,169	215,000
2	9	5_6	270,633	0,029	2 159,598	50,000	90,211	239,955
2	10	11_12	270,633	0,029	2 159,598	50,000	90,211	239,955
2	11	6_0	324,760	0,022	2 291,447	60,000	108,253	254,605
2	12	12_0	324,760	0,022	2 291,447	60,000	108,253	254,605

APPENDIX D

Voltage drop calculation

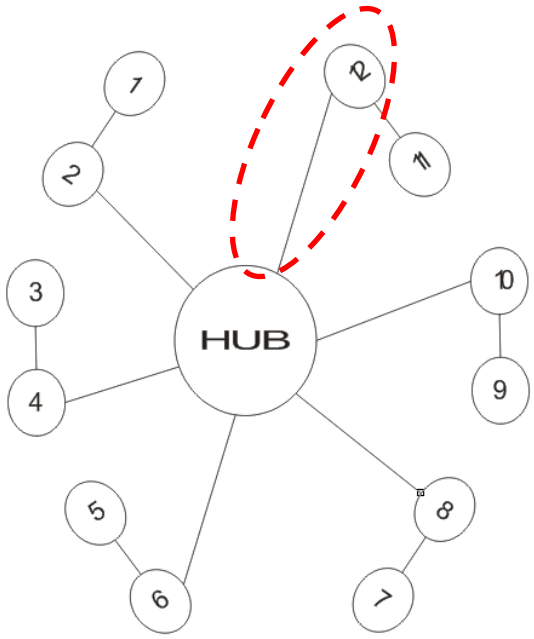

Let us consider a 6-radial system for instance. Here I am taking a single connection that is 12-HUB the data is as follows

$$\cos \emptyset = 0.8$$

$$\emptyset = \cos^{-1}(0.8) = 36.86°$$

$$U1 \ =?$$

$$U2 = \ 231\angle 36.86°V$$

$$U_1 = U_2 + I(R + jwL)$$

$$U_1 = 231\angle 36.86° + 108.25(0.083 + j0.016)$$

$$U_1 = 193.8 + j140.3\ V$$

$$U_1 = 239.25\angle 36°\ V$$

Here it can be easily seen that the angle is very small. Hence we can approximate our calculations to

$$U_1 = (R * I) + U_2$$

$$U_1 = (108.25 * 0.083) + 231$$

$$U_1 = 240.017\ V$$

$$\Delta U = 240.017 - 231$$

$$\Delta U = 9.01\ V$$

References

[1] "Waves4power," Waves4power, [Online]. Available: http://www.waves4power.se.

[2] A. Motors, "www.abb.com," [Online]. Available: http://www.abb.com/product/us/9AAC171953.aspx?country=SE.

[3] ABB, *ACSM1-204 Hardware Manual, "EN_ACSM1_204_HW_A".*

[4] ABB, *Hardware Manual ACS850-04 Drive module.*

[5] L. Rodrigues, "Wave power conversion systems for electrical energy production".

[6] IMechE, *Wave Energy paper,* European Directory of Renewable Energy , 1991.

[7] C. Boström, "Electrical systems for wave energy conversions," Uppsala University, 2011.

[8] S. Generators. [Online]. Available: http://itee.uq.edu.au/~mmme2104/Lecture%207%20-%20Synchronous%20Generators.pdf.

[9] M. G. Simões, S. Chakraborty and R. Wo, "Induction Generators for Small Wind Energy," IEEE Power Electronics Society, 2006.

[10] T. Lipo, "Synchronous reluctance machine, A viable alternative for AC Drives.," 1991.

[11] A. Vagati, "THE SYNCHRONOUS RELUCTANCE SOLUTION:A NEW ALTERNATIVE IN A.C. DRIVES," Vols. 0-7803-1328-3/94, no. IEEE, 1994.

[12] S. m. I. M. P. Aldo Boglietti, "Induction and synchronous reluctance motors comparison," no. IEEE, 2008.

[13] E. Cortina and m. b. A. Sfyrla, *Diodes,* University of Geneva.

[14] A. Sattar, "Insulated gate bipolar transistor (IGBT) basics," no. IXYS Corporation.

[15] Z. Xi, D. Domes and R. Rupp, "Efficency improvement with silicon carbide based power modules".

[16] D. C. Miesner, D. R. Rupp, H. Kapels, M. Krach and D. I. Zverev, "thinQ!™ Silicon Carbide

Schottky Diodes: An SMPS Circuit Designer’s Dream Comes True!".

[17] M. O´Neill, "SiC puts new Spin on Motor Drives," January 2005.

[18] K. Thorburn, H. Bernhoff and M. Leijon, "Wave energy transmission system concepts for linear generator arrays," *Ocean Engineering,* pp. 1339-1349, 20 Feburary 2004.

[19] SEEWEC, "Deliverable D10b part 2, subtask 2: Design and evaluation of electrical collection and transmission system for wave energy park," 2006.

[20] U. Cables, "www.universalcables.biz," [Online]. Available: http://www.universalcables.biz/images/price%20list.pdf.

[21] J. Manwell, J. Mcgowan and A. Rogers, Wind Energy Explained, Second ed., Wiley, 2009, pp. 422-428.

[22] VATTENFALL, *Kentish Flats Offshore Windfarm.*

[23] IEC, *IEC 60502-1,* Geneva: PRICE CODE, 2004.

[24] U. Cables, "http://www.ucable.com.," [Online]. Available: http://www.ucable.com.my/images/products/UC%20XLPE%20Catalogue.pdf.

[25] B. Drew, A. R. Plummerr and M. N. Sahinkaya, "A review of wave energy converter technology," 2009.

[26] R. W. Carter, *Wave energy converters and a submerged horizontal plate,* 2005.

[27] D. Larruskain, I. Zamora, A. Mazón, O. Abarrategui and J. Monasterio, "Transmission and Distribution Networks: AC versus DC".

[28] Siemens, "High Voltage Direct Current Transmission".